Title: Genetic differentiation and adaptive evolution of buff-tailed bumblebees in Asia

Authors:

Long Su[1], Lele Ding[2], Paul H. Williams[3], Yan Liu[1], Ruijuan Wang[1], Xiaoyan Dai[1], Shan Zhao[1], Haolin Fu[1], Xiaomeng Zhao[4], Quangui Wang[5], Yancan Li[1], Huiling Sang[6], Robert M. Waterhouse[7], Yifan Zhai[1]*, Cheng Sun[8]*

Affiliations:

[1]Institute of Plant Protection, Shandong Academy of Agricultural Sciences, Jinan, China

[2]College of Environmental and Resource Sciences, Zhejiang University, China

[3]Department of Life Sciences, Natural History Museum, London, United Kingdom

[4]College of Animal Science, Shanxi Agricultural University, Taigu, Shanxi, China

[5]Changping Laboratory, Beijing, 102206, China

[6]School of Biological Sciences, Victoria University of Wellington, Wellington, New Zealand

[7]Department of Ecology and Evolution, University of Lausanne, and SIB Swiss Institute of Bioinformatics, 1015 Lausanne, Switzerland

[8]College of Life Sciences, Capital Normal University, Beijing, China

***Corresponding authors:** Cheng Sun (cheng.sun@cnu.edu.cn) & Yifan Zhai (saaszyifan@163.com).

Keywords: *Bombus terrestris*, population genomics, adaptation, positive selection

Abstract

Bumblebees are ecologically and economically important pollinating insects, so their declines resulting from environmental changes have received intensive attention. Understanding how environmental factors shape the genetic differentiation of natural populations and identifying the genetic basis of local adaptation will provide insights into how species may cope with environmental changes. The buff-tailed bumblebee (*Bombus terrestris*) has a wide natural distribution range and has been successfully domesticated to produce commercial colonies for greenhouse pollination. Previous population genetics studies on *B. terrestris* have mainly focused on populations in Europe; however, populations in Asia, representing the eastern side of its natural distribution, have been less thoroughly sampled. To fill this gap, we collected wild *B. terrestris* samples from Asia, as well as wild *B. terrestris* from Europe and samples from domesticated colonies. We conducted whole-genome resequencing for 77 collected *B. terrestris* workers and performed population genomics analysis. Our results revealed significant genetic differentiation (F_{ST}= 0.076) between buff-tailed bumblebees in Europe and Asia, along with notable morphological and physiological differences. Consequently, *B. terrestris* in Asia represents a distinct new genetic resource. Demographic analysis suggested that the population size of buff-tailed bumblebees had increased during historic cold periods, confirming their cold-adapted characteristics. Selective sweep analysis identified 331 genes under selection in the genomes of Asian *B. terrestris*, likely involved in their adaptation to high ultraviolet radiation, low temperature, and low precipitation in their habitats. Our research provides insights into the population genetic structure and genetic basis of local adaptation in the buff-tailed bumblebee, which will be useful for its conservation and management.

Introduction

Bumblebees (genus *Bombus*) are ecologically and economically important pollinating insects, with ~250 extant species worldwide (Williams, 1998). They have long been known as excellent pollinators of greenhouse tomato crops, decreasing the cost of labor and improving the yield and quality of the fruits (Velthuis & Doorn, 2006). Today their pollination services have been extended to various other crops grown in poly-tunnels and open fields (Velthuis and van Doorn 2006; Garibaldi et al., 2013; Martin et al., 2019). Bumblebees are also ecologically important pollinators, serving as the sole or predominant pollinators of large numbers of wild plants (Fontaine et al. 2006; Goulson et al. 2008).

However, the declines of bumblebees in abundance and distribution, caused by global and local environmental changes, pose a threat to both wild plants and crop pollination (Williams et al., 2009; Cameron et al., 2020). This decline has raised concerns regarding the implications for bumblebees, food security, and ecosystem stability (Bartomeus et al., 2013; Cameron and Sadd 2020; Soroye et al. 2020). Understanding how environmental factors shape the genetic differentiation of natural populations and identifying the genetic basis of local adaptation will provide insights into how species respond to environmental changes, which is fundamental to bumblebee conservation and breeding (Hoffmann and Sgrò, 2011; Franks and Hoffmann, 2012; Savolainen et al., 2013; Sang et al., 2024).

The buff-tailed bumblebee, *Bombus terrestris* (Linnaeus, 1758), is one of the most widely used pollinator species for greenhouse crop pollination, and has been artificially reared by commercial companies since the 1980s (Velthuis and Van Doorn 2006; Goulson, 2010). *Bombus terrestris* is abundant in the West Palearctic regions, with a natural distribution that includes Atlantic islands, North Africa, Mediterranean islands, continental Europe, the south Ural Mountains, and extending east to the Altai Mountains (as far east as Mongolia) (Estoup et al., 1996; Rasmont et al., 2008; Williams et al., 2012). Therefore, *B. terrestris* is a broadly distributed species and exposed to diverse climatic conditions, which makes it a good model to study

population differentiation and local adaptation.

Several studies have been performed to understand the population genetic structure and differentiation of *B. terrestris*, mainly focused on European and nearby Mediterranean and Atlantic Island populations (Moreira et al., 2015; Kraus et al., 2009; Lecocq et al., 2013; Estoup et al., 1996; Widmer et al. 1998; Silva et al., 2020; Colgan et al., 2022). However, *B. terrestris* populations in Asia, representing the eastern edge of its global natural distribution, have been sampled only for morphological and COI barcode variation analyses (Williams et al., 2012).

To address in this gap, we collected wild *B. terrestris* samples from 11 Asian geographic populations, located an average distance of 5,100 kilometers from mainland Europe. Wild samples from Europe and domesticated samples from a commercial company were also collected. Whole-genome resequencing was performed on these samples, generating data for population genomic analyses to infer the population genetic structure and demographic history of *B. terrestris* and to identify candidate genes involved in the local adaptation to its Asian habitats.

Materials and Methods

Sample collection

Buff-tailed bumblebee (*B. terrestris*) samples were collected from both Asia and Europe for whole-genome resequencing. More specifically, 41 wild samples were collected from 9 geographic sites in Xinjiang, China, with an average distance of 254 kilometers between each site (Table S1). Additionally, 12 wild specimens were obtained from the Natural History Museum, London, United Kingdom, which originated from 6 European countries (France, Germany, Sweden, Switzerland, Turkey, England) and 3 Asian regions (Tajikistan, Kyrgyzstan, Russia (82.93N 55.01E)) (Table S1). Moreover, 24 commercial (domesticated) *B. terrestris* samples were also used. These samples were purchased from KOPPERT, a Netherlands-based company that has been involved in the breeding and domestication of buff-tailed bumblebees for over 35 years.

114 **Phenotypic characterization**

115 Phenotypic traits of *B. terrestris* were measured using a stereomicroscope and
116 the Micro Measurement and Data Analysis System (v1.01). These traits included
117 proboscis length, forewing length (FL), forewing width (FB) , cubital vein A, cubital
118 vein B, wing vein angles (A4, B4, D7, E9, G18, J10, J16, K19, L13, N23, O26, new
119 angle), hooks on the right hind wing, femur length (Fe) of the right hind leg, tibia
120 length (Ti) of the right hind leg, metabasitarsus length (ML), metabasitarsus width
121 (MT), length of the third abdominal sternum (S3), width of the third abdominal
122 sternum, width of the fourth abdominal sternum, length of the genitalia, and width of
123 the genitalia.

124 To measure hair density on the face and mesothorax of buff-tailed bumblebees,
125 we selected three representative areas of approximately 0.4 mm^2 and counted the
126 puncture density in each area. In some cases, particularly for specimens with high hair
127 density or hairs that formed clumps due to handling during capture and/or
128 preservation, hairs at their insertion points (usually indicated by a micropore on the
129 cuticle) were counted. An additional advantage of counting micropores is that it could
130 be applied to specimens that have lost hairs (e.g., due to aging; Bosch & Vicens, 2006;
131 Southwick, 1985; or poor handling) to obtain a measure of the original hair coverage.

132 Using the SUN-V Intelligent Insect Supercooling Point Tester (SUN Company,
133 Jinan, China), supercooling points of *B. terrestris* individuals from different sampling
134 sites were determined. Phenotypic data were correlated with supercooling point data
135 for association and difference analysis.

136 **DNA extraction**

137 Prior to DNA extraction, all buff-tailed bumblebee samples underwent surface
138 cleaning with alcohol. DNA extraction was performed using the QIAGEN Gentra
139 Puregene Tissue Kit (QIAGEN, Germany) following standard protocols. Given that
140 museum specimens may have suffered DNA damage (Dabney et al., 2013), DNA
141 repair was conducted on DNA extracted from those samples using the NEBNext
142 FFPE DNA Repair Mix kit (New England Biolabs, NEB). In total, 77 genomic DNA

143 samples of buff-tailed bumblebees were successfully obtained for downstream
144 sequencing and analysis.

145 **DNA barcoding analysis**

146 To verify the identity of the samples as *B. terrestris*, a barcoding PCR
147 experiment was conducted following the protocol outlined by Hebert et al. (2004).
148 The PCR primers were LEPr (TAAACTTCTGGATGTCCAAAAAATCA) and LEPf
149 (ATTCAACCAATCATAAAGATATTGG). The reaction mixture (15 μL) consisted
150 of 10× Buffer with 15 mmol/L $MgCl_2$ (1.5 μL), 10 mmol/L dNTPs (0.3 μL), each
151 primer at 15 μmol/L concentration (1.0 μL each), Taq polymerase (5 U/μL) (0.2 μL),
152 25 ng/μL DNA template (2 μL), and ddH_2O (10.725 μL).

153 PCR cycling conditions were as follows: initial denaturation at 95 °C for 5
154 minutes, followed by 33 cycles of denaturation at 94 °C for 30 seconds, annealing at
155 56 °C for 30 seconds, extension at 72 °C for 30 seconds, and a final extension at
156 72 °C for 5 minutes. The PCR products then underwent Sanger sequencing to obtain
157 barcoding sequences. Finally, sequences of the 77 samples were submitted to the
158 BOLD Systems website (http://www.boldsystems.org/index.php) for species
159 identification.

160 **Genome resequencing and read mapping**

161 Genomic DNA quality and integrity were assessed using a nucleic acid analyzer
162 and agarose gel electrophoresis. DNA samples of high quality, with good integrity and
163 minimal degradation, were randomly fragmented. Libraries for paired-end sequencing
164 were constructed according to Illumina sequencing platform requirements.
165 Sequencing was performed using the Illumina HiSeq 2000 sequencer, generating
166 paired-end sequencing reads with a length of 150 base pairs (bp). Additionally,
167 because some wild samples were museum specimens, to mitigate the effects of
168 depurination reactions that may have occurred during storage of museum specimens,
169 we trimmed two bases from both ends of each read using FASTQ software.

170 **Variant calling**

171 Genomic sequencing data from *B. terrestris* samples were aligned to the
172 reference genome (assembly Bter_1.0 GCA_000214255.1 (Sadd et al., 2015)) using

173 BWA-MEM software (Li and Durbin, 2009) with default parameters. The resulting
174 alignments were converted into BAM format using SAMtools (Li et al., 2009) and
175 sorted accordingly. Duplicate reads were removed using the GATK MarkDuplicates
176 module (McKenna et al., 2010). Sequencing depth and coverage were then evaluated
177 using SAMtools and BEDtools (Quinlan and Hall, 2010). For variant calling
178 (including Single Nucleotide Polymorphisms: SNPs and Insertions-Deletions:
179 INDELs), the GATK tools HaplotypeCaller, CombineGVCFs, GenotypeGVCFs, and
180 SelectVariants were utilized. The obtained variants then underwent rigorous filtering
181 using the GATK VariantFiltration module.SNP; variant annotations were conducted
182 using ANNOVAR (Wang et al., 2015) and SnpEff (Cingolani et al., 2012).

183 **Kinship analysis**

184 High genomic homogeneity among individuals from the same colony or closely
185 related bees can lead to errors in population genomics analysis. To address this, we
186 employed the KING-robust method (Manichaikul et al., 2010) using SNP information
187 across the whole genome to compute pairwise kinship coefficients among the 77
188 samples. Since in most bumblebees, queens mate once with a single male while males
189 can mate with multiple queens (Boomsma and Ratnieks, 1996; Nasei et al., 1998;
190 Schmid-Hempel and Schmid-Hempel, 2000), we applied such parameters in the
191 KING software. Individuals with kinship coefficients greater than 0.354 were
192 considered full siblings, while those with coefficients between 0.177 and 0.354 were
193 considered half-siblings. Therefore, during sample filtering, individuals with kinship
194 coefficients greater than or equal to 0.177 were treated as belonging to the same
195 colony, and only one individual per colony was retained for subsequent analyses. This
196 resulted in a total of 67 individuals being retained for downstream analysis.

197 **Population genetic structure analysis**

198 To construct the phylogenetic tree of *B. terrestris* samples, we used *Bombus*
199 *ignitus*, which belongs to the same subgenus as *B. terrestris*, as an outgroup (Williams
200 et al., 2008). The *B. ignitus* data were downloaded from the National Center for
201 Biotechnology Information (NCBI) (PRJNA659133, (Sun et al., 2020)).
202 Genome-wide SNP data from 67 *B. terrestris* samples and one *B. ignitus* sample were

203 turned to phylip files using Plink software (Chang et al., 2015). The data was then
204 used to build a Maximum Likelihood tree with RAxML (Randomized Axelerated
205 Maximum Likelihood) software (Stamatakis, 2014). Bootstrap analysis with 1,000
206 replicates was performed, and a RAxML_bestTree was generated. The final
207 phylogenetic tree was visualized using FigTree software
208 (http://tree.bio.ed.ac.uk/software/figtree/).

209 Principal component analysis (PCA) was conducted on genome-wide SNP data
210 from 67 *B. terrestris* samples. The data were first formatted into ped and map files
211 using Plink software. PCA analysis was performed using the smartPCA module
212 within EIGENSOFT software (Patterson et al., 2006). The results were visualized
213 using scatter plots generated with the ggplot2 package in R.

214 Using structure analysis, we employed a maximum likelihood estimation
215 algorithm assuming Hardy-Weinberg equilibrium. Structure assigns *B. terrestris*
216 samples to distinct populations or admixed groups based on their genetic variation.
217 This approach offers insights into the genetic composition and admixture patterns
218 across various values of K, shedding light on the evolutionary history of *B. terrestris*
219 populations. The results from the Structure analysis were visualized using the ggplot2
220 package in R, aiding in the interpretation of clustering patterns and genetic admixture
221 among individuals.

222 **Gene flow tests**

223 The ABBA-BABA test, also known as a D-test (D-statistics), is a widely used
224 method in population genetics to detect significant deviations caused by admixture
225 events. To examine gene flow between Asian wild populations, European wild
226 populations and the commercial (domestic) populations of *B. terrestris*, the
227 ABBA-BABA test was employed, with the use of *B. ignitus* as the outgroup. The
228 analysis included two main combination models: ((Wild-Europe, Domestic),
229 Wild-Asia, Outgroup) and ((Domestic, Wild-Europe), Wild-Asia, Outgroup). These
230 models were cross-validated to ensure the robustness of the results. Z-scores with
231 absolute values greater than 3 indicate statistically significant gene flow.

232 TreeMix analysis using whole-genome allele frequency data was then used to
233 infer population splits and admixture events (Pickrell and Pritchard, 2012). To detect
234 gene flow among different populations of *B. terrestris*, TreeMix analysis was also
235 employed on the 67 *B. terrestris* samples, using *B. ignitus* as the outgroup. Wild
236 populations of *B. terrestris* were grouped by country of collection (France, Germany,
237 Sweden, Switzerland, Turkey, United Kingdom, Tajikistan, Kyrgyzstan, Russia, and
238 China) to examine gene flow patterns between countries.

239 **Pairwise sequentially Markovian coalescent (PSMC) analysis**

240 The PSMC model (Li and Durbin, 2011) is a method used to estimate the time to
241 the most recent common ancestor by assessing the density of heterozygous sites
242 across a diploid genome. In our study, we utilized the PSMC model to estimate
243 historical population changes in Asian and European populations. Given the stringent
244 requirements of this analysis for sequencing depth (>20×) and extensive coverage,
245 low-quality sequencing data may introduce inaccuracies. To ensure robust outcomes,
246 we utilized 41 high-quality resequencing datasets for ***B. terrestris*** samples collected
247 from Xinjiang of China to represent the Asian population and 14 high-quality
248 resequencing datasets from commercial (domesticated) ***B. terrestris*** samples bought
249 from one European company to represent the European population.

250 To correlate the historical dynamics of ***B. terrestris*** populations with past climatic
251 conditions, we analyzed how the population size of bumblebees was influenced by
252 climatic changes. We employed mass accumulation rates (MAR) of loess deposits
253 from the Loess Plateau over the past three million years as a proxy for global
254 historical temperature changes (Sun and An, 2005). MAR values serve as indicators
255 of global climate patterns: while lower MAR values correspond to warm and humid
256 climates, higher values indicate cold and arid conditions.

257 **Analysis of climatic data**

258 We analyzed climatic data from sampling points of 15 wild Asian bumblebees
259 and 9 wild European bumblebees based on their geographic coordinates. Using
260 ArcMap (version 10.2), climatic data for each sampling point were obtained from the
261 WorldClim database (https://www.worldclim.org/). The main climatic variables

262 included minimum temperature, annual mean temperature, maximum temperature,
263 precipitation, elevation, and solar radiation. All climatic data were categorized into
264 two groups based on geographic coordinates: Asia and Europe. Subsequently, we used
265 R to conduct Wilcoxon rank-sum tests on each climatic variable to assess if there
266 were any significant differences between the Asian and European population
267 locations.

268 **Detection of positive selection in Asian *B. terrestris* populations**

269 41 *B. terrestris* specimens collected from Xinjiang, China and three specimens
270 collected from Tajikistan, Kyrgyzstan, and Russia represent the Asian population
271 (collection sites in red color in Figure 1A). The European population included 9 *B.*
272 *terrestris* specimens collected from France, Germany, Sweden, Switzerland, Turkey,
273 and the United Kingdom (collection sites in green color in Figure 1A), along with one
274 individual of domesticated *B. terrestris* bought from a European company.

275 To identify selected genomic regions in the Asian population, we employed three
276 metrics: 1) the ratio of genetic diversity between European and Asian populations
277 (ln-ratio $_{\pi Europe/\pi Asia}$); 2) the population differentiation coefficient F_{ST} between
278 European and Asian populations; and 3) the Composite Likelihood Ratio (CLR)
279 values in Asian the population. The ratio of genetic diversity and the population
280 differentiation coefficient F_{ST} were calculated with vcftools (versions 4.2) (Danecek
281 et al., 2011) using a sliding window approach, with a window size of 10 kb and a step
282 size of 5 kb. CLR values were calculated with SweeD (Pavlidis et al., 2013) using a
283 grid size of 1 kb. Based on results from the above two analyses, genetic diversity
284 ratios (ln-ratio $_{\pi Europe/\pi Asia}$), F_{ST} values, and CLR values were ranked to identify
285 genomic regions falling within the top 5% for all these three metrics, which were
286 deemed as regions putatively under selection in the Asian *B. terrestris* population.

287 **Functional prediction of focal genes**

288 To predict the functions of genes under selection in the Asian population, we first
289 identified the genomic locations of these genes using the genome annotation file
290 (Annotation Release 102). Subsequently, we extracted their amino acid sequences and
291 used InterProScan software (Jones et al., 2014) to assign Gene Ontology (GO) terms

292 for each protein-coding gene. The results of the GO annotation were then subjected to
293 enrichment analysis using the R Package TopGO (Alexa et al., 2024). In addition, we
294 utilized the Kyoto Encyclopedia of Genes and Genomes (KEGG) Orthology Based
295 AnnotationSystem (KOBAS) (Xie et al., 2011) to perform KEGG pathway annotation
296 and enrichment analysis for these genes. Finally, we performed BLAST searches
297 using the amino acid sequences of these genes against the fruit fly database, FlyBase
298 (Marygold et al., 2016), to identify homologous genes in *Drosophila*. Through this
299 approach we could infer potential functions of these *B. terrestris* genes based on their
300 counterparts in fruit flies.
301

302 # Results

303 **Genome resequencing of buff-tailed bumblebees collected from Europe and Asia**

304 A total of 77 *B. terrestris* samples were collected from Asia and Europe for this
305 analysis (Fig. 1A). Specifically, 41 wild samples were collected from 9 locations
306 within Xinjiang province, China, with an average distance of 254 kilometers between
307 collection sites. 12 additional wild samples were obtained from the Natural History
308 Museum London (https://www.nhm.ac.uk/), which were specimens collected from 6
309 countries in Europe (France, Germany, Sweden, Switzerland, Turkey, and England)
310 and 3 Asian regions (Tajikistan, Kyrgyzstan, and Russia (82.93N 55.01E)) (Table S1).
311 The identity of all these wild samples was confirmed by DNA barcoding (Hebert et al.
312 2004). In addition to the wild samples, 24 commercial (domesticated) *B. terrestris*
313 samples were included in this study, which were bought from *KOPPERT* - a company
314 based in the Netherlands.

315 We performed whole-genome resequencing for these samples and achieved a
316 mean depth of coverage of 30.80× and mean breadth of coverage of 99.37% (Table
317 S2). Notably, specimens from the Natural History Museum London yielded an
318 average depth of 20.99× (ranging from 11.3× to 33.74×) and a mean breadth of
319 coverage of 98.94% (ranging from 96.9% to 99.54%) (Table S3). The Genome
320 Analysis Toolkit (Mckenna et al., 2010) software was used to call variants for these

77 buff-tailed bumblebees, and a total of 4,827,687 high-quality single nucleotide polymorphisms (SNPs) and 615,899 high-quality insertion-deletions (INDELs) were obtained. Based on the obtained SNPs, we estimated kinship coefficients for these bumblebees and found that 10 commercial samples were full-or-half-sisters to other individuals (1st degree sibling: 0.177-0.354; Manichaikul et al., 2010). Therefore, we excluded these 10 samples and a total of 67 buff-tailed bumblebees were retained for downstream analysis.

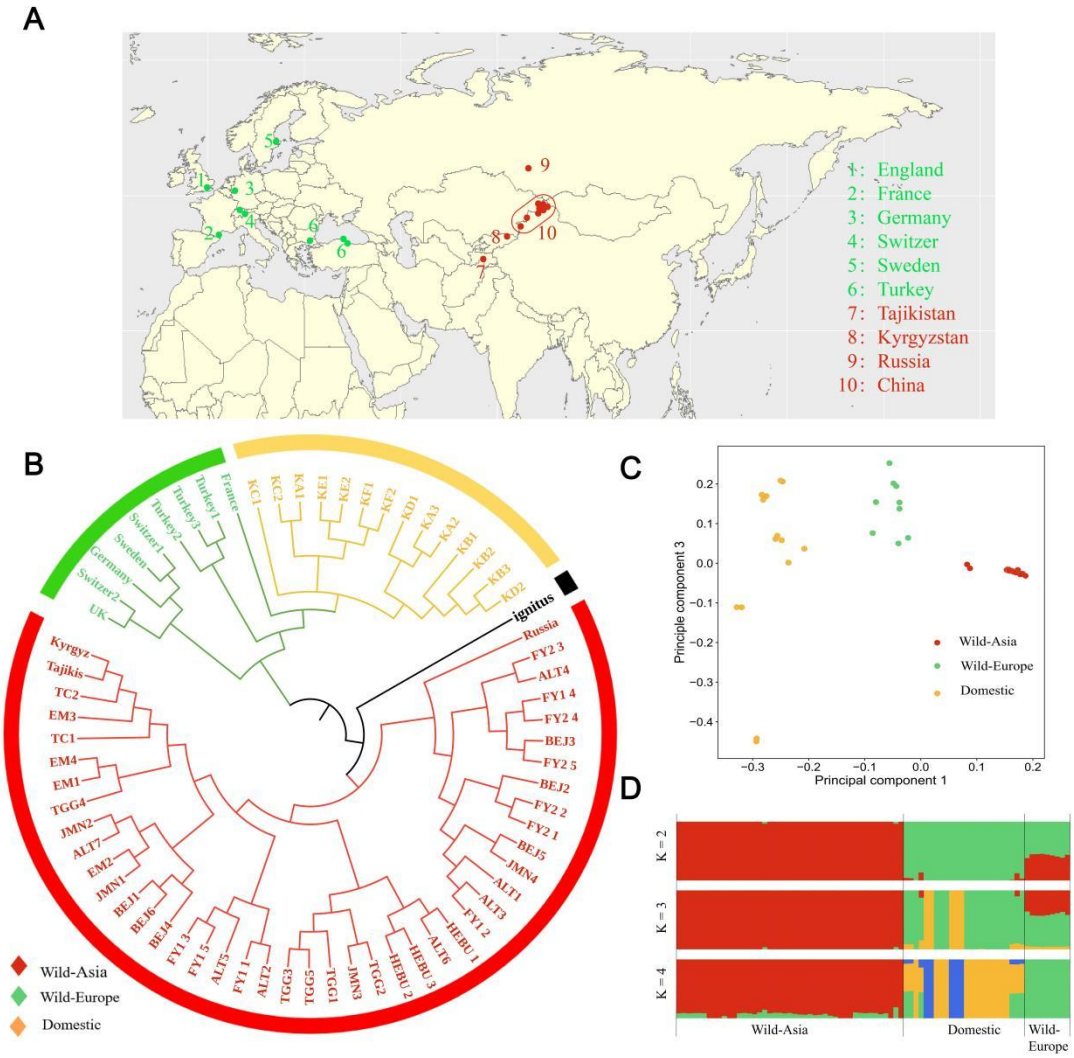

Fig1. Sampling sites and population genomic analyses of *Bombus terrestris* individuals sampled from across Asia and Europe. (A) Geographic locations of the 53 wild-sampled *B. terrestris* individuals (red: collection sites in Asia, green: collection sites in Europe). (B) Maximum likelihood phylogenetic tree based on SNPs using *B. ignitus* as the outgroup, (C) Principal component analysis (PCA) plot showing wild-Asian (red), wild-European (green), and domestic (yellow) samples on PC1 and PC3, and (D) STRUCTURE analysis results (K = 2 - 4) for 67 of the 77 wild and domestic *B. terrestris* individuals (10 domestic samples excluded based on kinship analysis results).

Distinct genetic differentiation exists between Asian and European buff-tailed

337 **bumblebees**

338 To understand the genome-wide relationships and divergence between different
339 *B. terrestris* samples, we constructed the maximum likelihood (ML) tree using these
340 67 resequenced individuals, using *Bombus ignitus* (belonging to subgenus *Bombus*) as
341 the outgroup (Fig. 1B, Fig. S1).

342 The phylogenetic tree based on genome-wide SNPs revealed that the 67 *B.*
343 *terrestris* individuals could be divided into two groups: 1) the first group, named as
344 Wild-Asia, consisted of 44 wild *B. terrestris* samples collected from China, Tajikistan,
345 Kyrgyzstan, and Russia; 2) the second group comprised 9 wild samples collected
346 from France, Germany, Sweden, Switzerland, Turkey, and England (named as
347 Wild-Europe) and 14 domesticated samples (named as Domestic) (Fig. 1B). In
348 addition, the close relationship observed between the Domestic and Wild-Europe *B.*
349 *terrestris* samples (Fig. 1B) was consistent with the fact that the commercial *B.*
350 *terrestris* colonies have been domesticated from wild *B. terrestris* in Europe (Velthuis
351 and Van Doorn 2006). The relationships inferred from the phylogenetic analysis were
352 supported by Bayesian clustering analysis using principal component analysis (PCA)
353 (Fig. 1C) and ADMIXTURE analysis (Fig. 1D). There was a clear genetic
354 differentiation between *B. terrestris* samples originating from Asia and those from
355 Europe.

356 To quantify the genetic differentiation between Asian and European *B. terrestris*,
357 we calculated pairwise F_{ST} values. The results showed that the pairwise F_{ST} value
358 between Wild-Asia and Wild-Europe was 0.076404 (Table. 1), indicating that there is
359 moderate genetic differentiation between them (Spitze, 1993).

360 **Buff-tailed bumblebees in Asia dispersed from Europe**

361 We calculated genetic diversity summary statistics and the results revealed that
362 the nucleotide diversity (π) value for the Wild-Europe group (π = 0.002906) was
363 higher than that of the Wild-Asia group (π = 0.002276), suggesting that buff-tailed
364 bumblebee populations in Europe are older than those of Asia (Table. 1). In addition,
365 Tajima's D test [Tajima's D (Wild-Europe) = -0.027101, Tajima's D (Wild-Asia) =
366 1.100971] (Table 1) suggested that buff-tailed bumblebees in Europe have a larger

367 population size than in Asia.

368

369 Table 1 Population genetic diversity summary statistics

Population	Pi	Tajima's D	F_{ST}	
			Wild-Asia	Domestic
Wild-Europe	0.003117	-0.02952	0.076122	0.060032
Wild-Asia	0.001877	1.8451	-	0.13277

370 To test the possibility that populations of Asian buff-tailed bumblebees were
371 impacted by the invasion of commercial *B. terrestris* colonies (imported from Europe),
372 we assessed gene flow between each population, specifically between the commercial
373 samples and the samples collected from Xinjiang province. Firstly, we used TreeMix
374 (Pickrell and Pritchard 2012) to infer the migration history among populations
375 (Wild-Asia, Wild-Europe, Domestic) by using the joint allele frequencies among all
376 populations in our study. TreeMix employs a maximum likelihood approach to model
377 the genetic relationships among populations and detect admixture events. Our analysis
378 did not reveal any gene flow between Domestic samples and Wild-Asia samples (Fig.
379 2); gene flow was found between Domestic samples and Wild-Europe samples, which
380 is expected as the former was domesticated from the latter; gene flow was also found
381 between Tajikistan and China-Xinjiang samples, which is expected as they are
382 geographically adjacent (Fig. 2A; Fig. 2B; Fig. 1A). To check the above gene flow
383 analysis between populations, we used the ABBA-BABA gene flow test. Results
384 confirmed that no gene flow was observed between Wild-Asia (Xinjiang) samples and
385 Domestic samples (Fig. 2C, 2D).

386 Finally, we calculated the geographic and genetic distances between wild *B.*
387 *terrestris* samples in Europe and Asia. We found that the genetic distance between
388 these samples follows a strict isolation-by-distance model ($R = 0.76$, $p < 2.2e-16$) and
389 a correlation between genetic distance and geographic distance was found among
390 individuals (Fig. 2E), suggesting that dispersal could explain the current genetic
391 distances between wild *B. terrestris* samples in Europe and Asia. Taken together, all
392 these findings suggest that buff-tailed bumblebees in Asia dispersed from ancestral
393 populations in Europe.

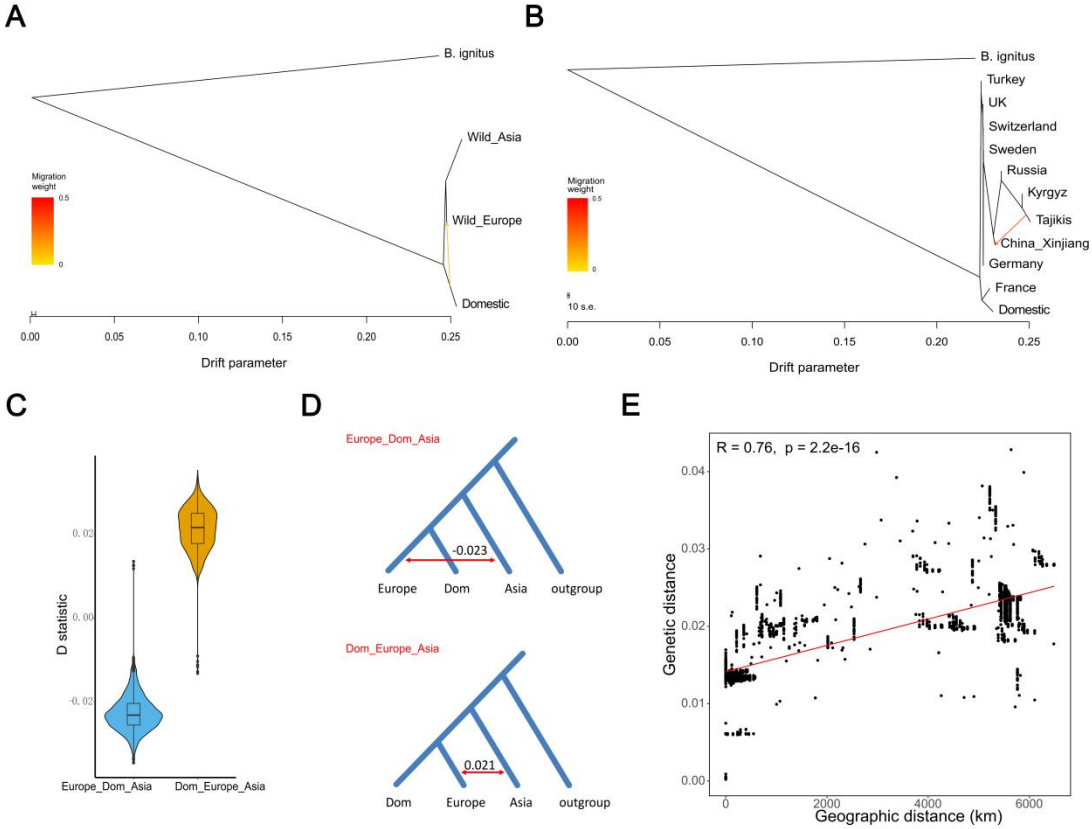

Fig2. Gene flow analysis for *B. terrestris* samples collected from different geographic locations. (A) TreeMix gene flow analysis between the three main *B. terrestris* groups. (B) TreeMix gene flow analysis between different collection sites. (C, D) Results from the ABBA-BABA gene flow test. The topology of Europe_Dom_Asia is (((Wild-Europe, Domestic), Wild-Asia), outgroup), and Dom_Europe_Asia is (((Domestic, Wild-Europe), Wild-Asia), outgroup). (E) Correlation analysis of genetic and geographic distances of *B. terrestris* samples.

The demographic history of buff-tailed bumblebees

Pairwise Sequentially Markovian Coalescent (PSMC) model (Li and Durbin 2011) analysis was employed to infer the historical effective population size (*Ne*) of buff-tailed bumblebees. Because this analysis has a high requirement for sequencing coverage, we used the 14 commercial *B. terrestris* samples to represent the European population and the 42 wild *B. terrestris* samples collected from Xinjiang province, China to represent the Asian population. The results (Fig. 3) indicated that buff-tailed bumblebees in Asia and Europe exhibited similar and relatively stable *Ne* until ~ 0.3 million years (Myr) ago. The population sizes of buff-tailed bumblebees in these two regions began to diverge at ~ 0.3 Myr ago, approximately at the onset of the Penultimate Glaciation (Zheng et al. 2002). After this, both buff-tailed bumblebee

populations exhibited an increasing *Ne* and *B. terrestris* in Europe showed a consistently higher *Ne* than that of Asia.

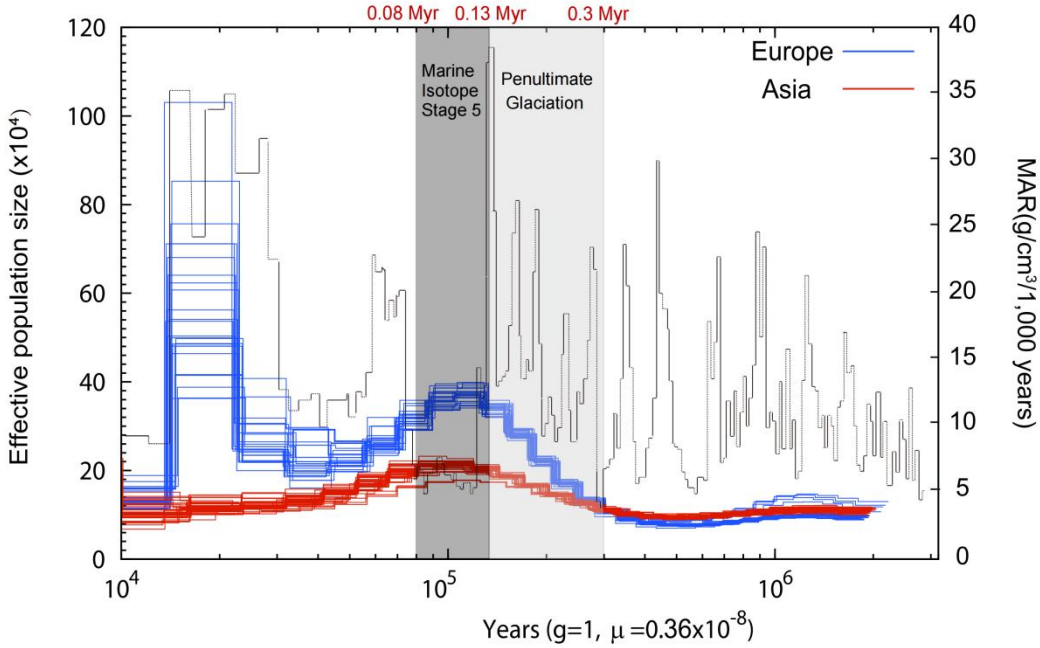

Fig3. Demographic history of Asian and European *B. terrestris* populations inferred by software PSMC (g=1,μ=0.36x10-8). The gray shading marks the Penultimate Glaciation (PG; 0.13 – 0.3 Myr). The gray line represents the mass accumulation rate (MAR) of the Loess Plateau: high MAR values indicating cold and dry conditions, while low MAR values indicating hot and wet conditions.

The gray line in Figure 3 represents the mass accumulation rate (MAR) of the Loess Plateau (Sun and An 2005), which serves as an indicator of climatic conditions, with high MAR values indicating cold and dry periods and low MAR values indicating hot and wet periods. Comparing the climate and effective population size estimates over time, we observed two main trends: 1) the increase in *Ne* between 0.13 Myr ago and 0.3 Myr ago coincided with the Penultimate Glaciation period (0.13–0.3 million years ago) (Zheng et al. 2002), when the climate became cold and dry; 2) During Marine Isotope Stage 5 (MIS5, 0.08 Myr to 0.13 Myr ago), a period characterized by hot and wet climate according to the MAR estimates, we observed a decrease in *Ne* for *B. terrestris* both in Europe and Asia. Therefore, we infer from the demographic analysis that changes in *Ne* of buff-tailed bumblebees are associated with historical climate changes, with an increasing *Ne* during cold periods and a declining *Ne* during hot periods.

Buff-tailed bumblebees in Asia and Europe differ in morphology and physiology

To understand if some environmental factors are significantly different between the two habitats (Europe and Asia) of buff-tailed bumblebees, we collated and compared the environmental factors of their habitats. Specifically, environmental data on temperature, elevation, solar radiation and precipitation were extracted from the global natural environment database (WorldClim) for the 24 *B. terrestris* collection sites in Europe and Asia. After comparison, we found several environmental factors were significantly different between the two habitats of *B. terrestris* (Fig. 4). Both the Mean and Minimum Temperatures of Asian habitats were significantly lower than that of European habitats ($p_{Ann\text{-}Mean\text{-}Temp}$=0.02942; $p_{Mean\text{-}Temp\text{-}Cold}$=0.02942; $p_{Min\text{-}Temp}$=0.009444). Additionally, the Elevation and Sun Radiation in Asian habitats were significantly higher than in European habitats ($p_{Elevation}$=0.007926; $p_{Sun\text{-}Radiation}$=0.004594). Moreover, the Precipitation in the Asian habitats was significantly lower than in European habitats ($p_{Precipitation}$=0.001733).

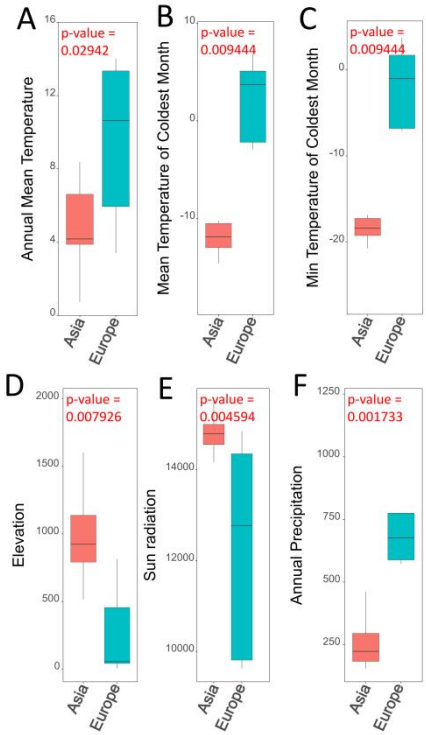

Fig4. The comparison of climate factors between the habitats of Asian and European *B. terrestris*, which include: (A) annual mean temperature, (B) mean temperature of coldest month, (C) minimum temperature of coldest month, (D) elevation, (E) solar radiation, and (F) annual precipitation. P-values from Wilcoxon rank-sum tests are indicated for each comparison.

To understand if buff-tailed bumblebees in the two habitats exhibit any

454 phenotypic differences, we measured and compared a selection of morphological
455 characters. We randomly selected Asian and European buff-tailed bumblebees from
456 different colonies and measured a set of features, including proboscis length, forewing
457 length (FL), forewing breadth (FB), cubital vein A, cubital vein B, wing vein angles
458 (A4, B4, D7, E9, G18, J10, J16, K19, L13, N23, O26, new angle), hooks on the right
459 hind wing, femur length (Fe) of the right hind leg, tibia length (Ti) of the right hind
460 leg, metabasitarsus length (ML), metabasitarsus breadth (MT), length of the third
461 abdominal sternum (S3), breadth of the third abdominal sternum, breadth of the fourth
462 abdominal sternum, length of the genitalia, breadth of the genitalia (Table S4). Results
463 indicated that buff-tailed bumblebees in Asia had a shorter proboscis length compared
464 to their European counterparts (Fig. 5B, 5E). The proboscis lengths of Asian queens
465 (n=10), workers (n=30), and males (n=15) were 9.75±0.44, 6.75±1.11, and 8.33±1.44,
466 respectively, while these lengths for European queens (n=10), workers (n=30), and
467 males (n=15) were 11.74±0.85, 9.24±0.81, and 10.03±0.72, respectively. We also
468 measured the hair density of the buff-tailed bumblebees, which refers to the number
469 of small pores within a 0.04-centimeter diameter area on a surface, and found Asian
470 samples exhibited a higher hair density (Fig. 5A, 5C, 5D, 5G). The hair densities on
471 the face and mesothorax of Asian bumblebees (n=30) were 775.1±39.6 and 863.4±
472 50.2, respectively, whereas those lengths for European bumblebees (n=30) were
473 675.97±78.75 and 594.5±53.56, respectively.

474 The ambient temperature in the Asian habitats of buff-tailed bumblebees was
475 lower than that of European buff-tailed bumblebees (Fig. 5F), so Asian *B. terrestris*
476 may have an enhanced capacity for cold tolerance. As the supercooling point and
477 freezing point were important parameters related to the survival of insects in cold
478 environments, we conducted measurements of the supercooling point and freezing
479 point for buff-tailed bumblebees in Asia and Europe. Results suggested that, as
480 expected, the supercooling point and freezing point of Asian buff-tailed bumblebees
481 were significantly lower than those of their European counterparts (Fig. 5F). The

supercooling point of *B. terrestris* in Asia was -10.17 ± 1.26 ℃ and the freezing point was -7.02 ± 1.5 ℃. In contrast, the supercooling point of European *B. terrestris* was -8.85 ± 1.04 ℃, with a freezing point of -5.58 ± 1.34 ℃.

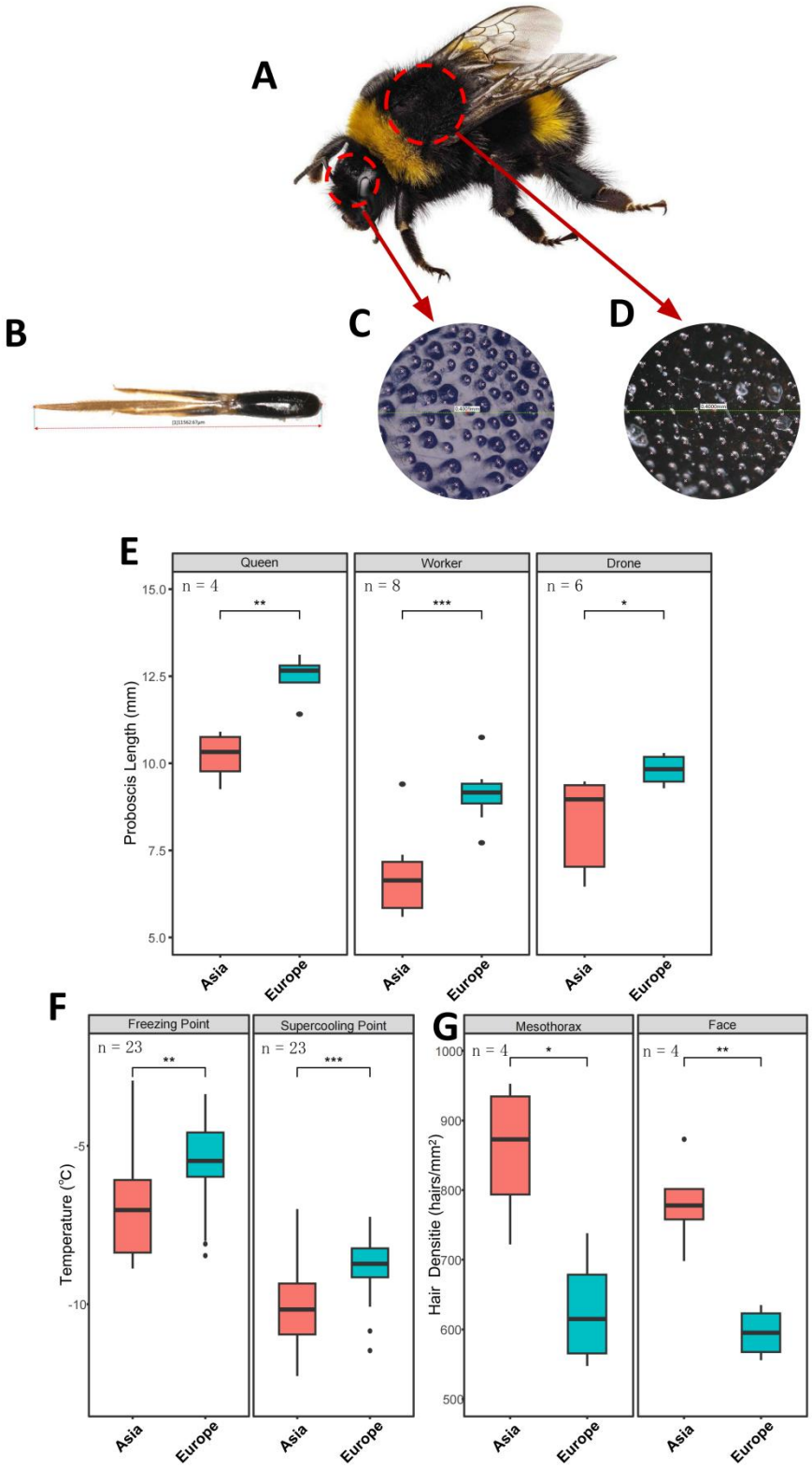

Fig5. The morphological and physiological differences detected between Asian and European *B. terrestris*. The overall appearance (A), proboscis (B), hair density on the face (C), and mesothorax (D), of Asian *B. terrestris*. (E) Comparative analysis of proboscis lengths for the queens, workers, and drones of Asian and European *B. terrestris*. (F) The freezing points and supercooling points of Asian and European *B. terrestris*. (G) The hair density on the face and mesothorax of Asian and European *B. terrestris*. P-values are indicated with *: $p<0.05$, **: $p<0.01$, ***: $p<0.005$.

Genomic signatures of local adaptation for buff-tailed bumblebees in Asia

The phenotypic and physiological differences observed in Asian buff-tailed bumblebees indicate that Asian *B. terrestris* have undergone local adaptation to their Asian habitats. To identify genomic regions that experienced positive selection in Asian *B. terrestris*, we performed whole-genome genetic differentiation analysis between Asian samples and European samples. We used the Sliding-Window method, with a window size of 10 kb and a step size of 5 kb, based on the top 5% for ln-ratio πEurope/πAsia (>0.6635) and fixation statistics F_{ST} (>0.196113) (Axelsson et al., 2013; Qiu et al., 2015). Our analysis yielded a total of 435 candidate genomic regions that were under positive selection encompassing ~ 6.64 Mb (2.64%) of the *B. terrestris* reference genome, with an average size of 15.2 Kb. Within these regions, there were 712 predicted protein-coding genes. To further refine this result, we employed the Composite Likelihood Ratio (CLR) test to identify genomic regions that were under selection. Candidate regions were extracted if they fell within the top 5% of Z-transformed values (>0.686) and they were identified as candidate regions under selection by the above ln-ratioπ and F_{ST} analysis. Applying these filters resulted in a total of 181 genomic regions being identified as under selection, within which there are 331 protein-coding genes (Table S7).

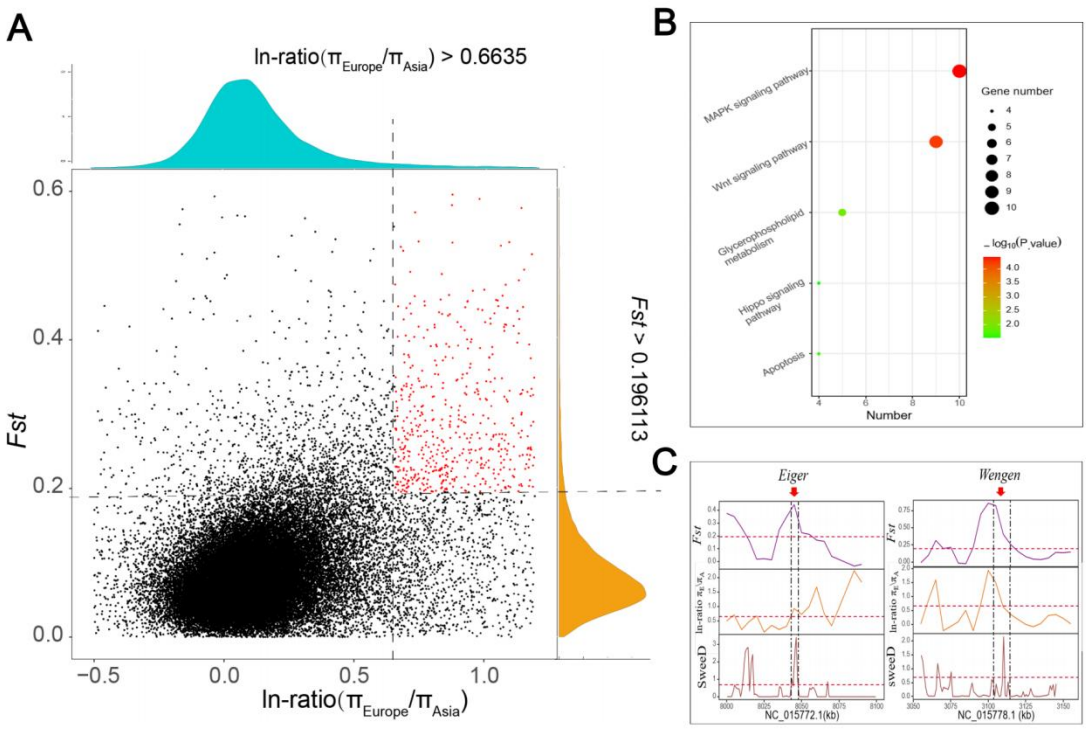

Fig6. Genomic regions and genes showing evidence of positive selection in Asian *B. terrestris*. (A) Distribution of ln-ratio π_{Europe}/π_{Asia} and fixation statistics F_{ST} of 10 kb windows with 5 kb steps. Red dots represent windows fulfilling the selected regions requirement (based on the top 5% for ln-ratio π_{Europe}/π_{Asia} (>0.6635) and fixation statistics F_{ST} (>0.196113)). (B) The plot shows the Gene Ontology (GO) categorization of identified genes in significant pathways (p <0.05). The color of the circle represents the $-\log$ P.value. The size of the circle represents the number of genes under selection in the enriched pathway. (C) Two focal genes – *Eiger* and *Wengen* - showing selection signals in Asian *B. terrestris*. ln-ratio π_{Europe}/π_{Asia}, F_{ST}, and SweeD (> 0.686) values are plotted using a 10kb sliding window.

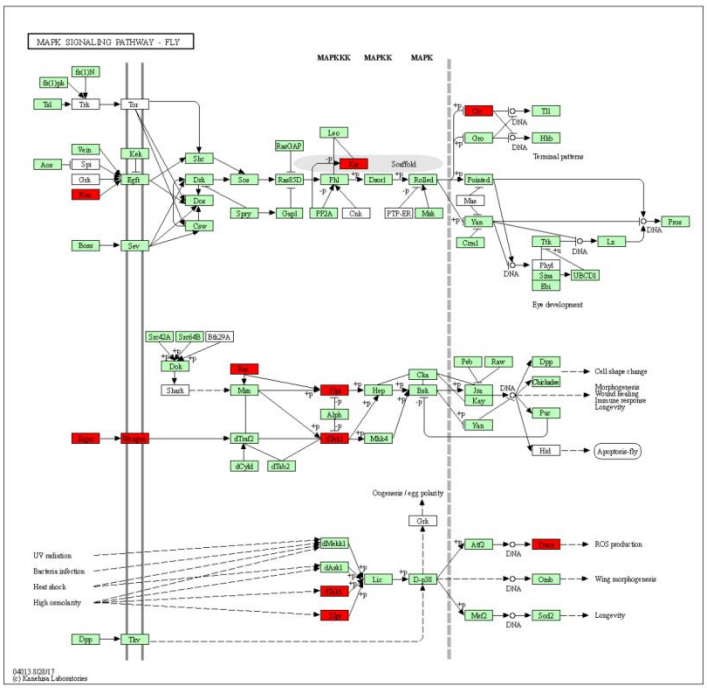

Fig7. The Kyoto Encyclopedia of Genes and Genomes (KEGG) pathway for MAPK signaling. Genes in the MAPK signaling pathway that exhibited patterns of positive selection in Asian *B. terrestris* are highlighted in red.

Discussion

The buff-tailed bumblebee (*B. terrestris*) is an important pollinator of wild plants and is one of the most widely used pollinator species for greenhouse crop pollination (Velthuis and Van Doorn 2006; Goulson, 2010). Intensive studies have been performed to understand its population structure, genetic differentiation and adaptation using samples from European and nearby Mediterranean and Atlantic Island populations (Moreira et al., 2015; Kraus et al., 2009; Lecocq et al., 2013; Estoup et al., 1996; Widmer et al. 1998; Silva et al., 2020; Colgan et al., 2022). However, less was known about *B. terrestris* populations in Asia, which represent the eastern edge of its global natural distribution (Williams et al. 2012). In this study, we collected wild *B. terrestris* samples from 11 geographic populations in Asia, as well as wild samples from Europe and domesticated samples from a commercial company in Europe. After whole-genome resequencing of these samples, we investigated their population genetic structure, demographic history and local adaptation.

Our results indicated that buff-tailed bumblebees could be divided into two groups: while samples originating from Asia were clustered into one group, samples originating from Europe were clustered into another group (Fig. 1). That is, previous studies on buff-tailed bumblebees largely missed the diversity represented by Asian populations. In addition, although *B. terrestris* in Asia most likely dispersed from European populations (Fig. 2; Fig. 3), distinct genetic differentiation was detected between the two groups (Table 1), with a F_{ST} value of 0.076404, indicating a moderate genetic differentiation (Spitze, 1993). Moreover, buff-tailed bumblebees in Asia and in Europe differ in morphology and physiology. For example, compared to their European counterparts, buff-tailed bumblebees collected in Asia (more specifically, Xinjiang province, China), had a shorter proboscis length, a higher hair density and a lower supercooling and freezing point (Fig. 5; Table S4). Taken together, considering the moderate genetic differentiation and distinct morphological and physiological differences,, buff-tailed bumblebees in Asia represent a distinct new

genetic resource.

Description of *Bombus terrestris* in Asia

Distribution: The species is mainly distributed in Asia in Iran, Russia, and the mountains of Central Asia and the northern Xinjiang region of China - areas of the Tianshan Mountains and the Altai Mountains, but also including western Mongolia.

Color Pattern: Consists of alternating bands of black and yellow on its body. The fore margin of thorax is covered in dense yellow hairs; the hind margin of abdomen is covered in white hairs; black elsewhere; corbicular cuticle and setae black.

Morphology: Morphological parameters of *B. terrestris* in Asia, including proboscis length, forewing length (FL), forewing width (FB), cubital vein A, cubital vein B, wing vein angles (A4, B4, D7, E9, G18, J10, J16, K19, L13, N23, O26, new angle), hooks on the right hind wing, femur length (Fe) of the right hind leg, tibia length (Ti) of the right hind leg, metabasitarsus length (ML), metabasitarsus breadth (MT), length of the third abdominal sternum (S3), width of the third abdominal sternum, width of the fourth abdominal sternum, length of the genitalia, breadth of the genitalia. Compared to the European bumblebees, *B. terrestris* in Asia have shorter proboscis length, higher hair density. All the morphometric characters are presented in supplementary Table S4, Supplementary Material online.

The local adaptation of buff-tailed bumblebees in Asia

Local adaptation is an important ability required for organisms to survive in changing environments (Fuse 2017). The dispersal of *B. terrestris* from Europe to Asia has encountered different environmental conditions, including those of temperature, elevation, and precipitation (Fig. 4). Correspondingly, *B. terrestris* in Asia exhibited altered phenotypes after occupying new environments, such as changes in proboscis length, increased hair density, and lower supercooling point (Fig. 5). It has been reported that plants at higher altitudes have smaller overall sizes of flowers (Ansari et al. 2010; Zhu et al. 2010; Halbritter et al. 2018; Kiełtyk et al. 2021). Therefore, flower sizes in *B. terrestris'* Asian habitats, which have a higher elevation (Fig. 4), should be smaller than in European habitats. Therefore, the shorter proboscis observed in *B. terrestris* in Asia could represent an adaptive trait for them to collect

582 food. Both mean and minimum temperatures of *B. terrestris'* habitat in Asia were
583 significantly lower than in Europe (Fig. 4). Bumblebees primarily rely on their body
584 hair to withstand low-temperature challenges (Heinrich et al. 1974), so the increased
585 hair density in *B. terrestris* in Asia could provide them with enhanced ability to
586 withstand cold temperatures. The phenomenon of supercooling refers to the ability of
587 insects to remain in a liquid state even when the temperature is below their freezing
588 point, which is widespread among insects and is crucial for their survival in cold
589 environments (Renault et al. 2002; Lombardo et al. 2017). A comparison between *B.*
590 *terrestris* in Asia and the European *B. terrestris* revealed that the former had a lower
591 supercooling point (Fig. 5), suggesting that *B. terrestris* in Asia is adapted to low
592 temperatures.

593 Genes related with local adaptation will show positive selection signals within
594 the genome. Here we employed a method that has been used in several organisms,
595 such as yaks (Qiu et al., 2015a), cows (Chen et al., 2018b), silkworms (Xia et al.,
596 2009), pigs (Rubin et al., 2012), soybeans (Zhou et al., 2015), and rice (Huang et al.,
597 2012), to identify genes under positive selection in *B. terrestris* in Asia. Our results
598 indicate that the MAPK pathway and glycerophospholipid (GPL) metabolic pathway
599 in *B. terrestris* in Asia had undergone selection (Table S6). Specifically, we observed
600 that *Eiger* and *Wengen* in these two pathways have been subjected to positive
601 selection (Table S7). Previous research has shown that *Eiger*, a homolog of tumor
602 necrosis factor in fruit flies, is released in epidermal cells undergoing apoptosis in
603 response to intense UV radiation; *Wengen*, on the other hand, acts as the receptor for
604 *Eiger* on sensory neurons, mediating the transmission of adaptive signals that enable
605 the organism to cope with UV radiation (Agrawal et al., 2016). Therefore, it is likely
606 that *Eiger* and *Wengen* contributed to the adaptation of *B. terrestris* in Asia to the
607 high-elevation and UV-intensive environments in their habitats. Additionally, studies
608 have demonstrated that *Eiger* can modulate insulin-mediated nutritional responses in
609 fruit flies, enhancing their adaptability to changing nutritional environments (Agrawal
610 et al., 2016). Considering the habitat characteristics of *B. terrestris* in Asia, such as
611 low precipitation, high elevation, and limited vegetation leading to reduced food

availability (Fig. 4), *Eiger* may play a role in enhancing Asian *B. terrestris'* adaptability to their nutritional environments. Genes in the glycerophospholipid (GPL) metabolic pathway were also found under positive selection (Table S6). Previous studies demonstrated the association between the glycerophospholipid (GPL) metabolism pathway and low-temperature adaptation in the hemipteran insect *Pyrrhocoris apterus* (Han et al., 1995; Tomcala et al., 2006). Also, it was reported that glycerophospholipids (GPL) play a crucial role in regulating the supercooling point in insects (Tomcala et al., 2006). Therefore, genes in the glycerophospholipid (GPL) metabolic pathway that showed selection signals likely enhanced the cold tolerance of *B. terrestris* in Asia.

Conclusion

Through collecting and re-sequencing buff-tailed bumblebees from their Asian habitats, which were less well represented in previous studies, we performed the first multi-locus population genetic structure analysis of this important pollinator. Our results revealed that buff-tailed bumblebees in Asia dispersed from Europe and accumulated a moderate genetic differentiation with their European counterparts. Buff-tailed bumblebees in Asia adapted to their habitats morphologically and physiologically and we identified genes that were likely involved in their adaptation to high UV radiation, low temperature, and low precipitation of their habitats. The new genomic resources and insights revealed through this study will be valuable for the conservation and improved management of this important pollinator.

Author contributions

C.S. and Y.Z. conceived and designed the study; P.H.W., L.S., C.S. and Y.Z. collected bee samples; L.S., D.L., Y.C.L., R. W., X. D., S.Z., H. F., X.Z., H.S. and Q.W. were involved in methodology; L.S., Y.C.L. collaborated on script compilation for data analysis; L.S. and C.S. drafted the initial manuscript; R.M.W., P.H.W. and Y.Z. gave guidance in the writing; all authors participated in reviewing and editing the

manuscript.

Acknowledgements

This work was supported by the National Natural Science Foundation of China (Grant No. 32270445 and 31971397), Swiss National Science Foundation (SNSF) (Grant numbers 202669 and 196125 to RMW), Shandong Provincial Natural Science Foundation (ZR2021YQ21, ZR2021QC218); Shandong Provincial Agriculture Research System (SDAIT-24); Taishan Scholars program of Shandong Province (tsqn202312293); Shandong Provincial Key R&D Program (2023LZGC017). This work was also supported by the Shandong Academy of Agricultural Sciences, Institute of Plant Protection, Shandong Key Laboratory for Green Prevention and Control of Agricultural Pests, Shandong Provincial Engineering Research Center for Development and Utilization of Beneficial Insects.

Competing interests:

The authors declare that they have no competing interests.

Data and Code Availability Statement:

All data and code will be made available upon acceptance.

References

Alexa A, Rahnenfuhrer J, 2024. TopGO: Enrichment analysis for gene ontology. R package version 2.56.0.

Agrawal N, Delanoue R, Mauri A, Basco D, Pasco M, Thorens B and L Opold P, 2016. The drosophila tnf eiger is an adipokine that acts on insulin-producing cells to mediate nutrient response. Cell Metab. 23(4):675-684.

Ansari S, Daehler C, 2010. Life history variation in a temperate plant invader, Verbascum thapsus along a tropical elevational gradient in Hawaii. Biological Invasions, 12:4033-4047.

Bartomeus I, Ascher J, Gibbs J, Danforth B, Wagner L, Hedtke, Winfree R, 2013. Historical changes in northeastern US bee pollinators related to shared ecological traits. Proc Natl Acad Sci U S A, 110(12):4656-4660.

Boomsma JJ, Ratnieks FL, 1996. Paternity in eusocial Hymenoptera. Philos. Trans. R. Soc. Lond. B Biol. Sci. 351(1342):947-975.

Cameron S, Hines H, Williams P, 2007. A comprehensive phylogeny of the bumble bees (Bombus). Biol J Linn Soc. 91(1):161-188.

Cameron S, Sadd B, 2020. Global Trends in Bumble Bee Health. Annu Rev Entomol. 65(209-232).

Chang CC, Chow CC, Tellier LC, Vattikuti S, Purcell SM, Lee JJ, 2015. Second-generation PLINK: rising to the challenge of larger and richer datasets. Gigascience. 4(1).

Chen N, Cai Y, Chen Q, Li R, Wang K, Huang Y, Hu S, Huang S, Zhang H, Zheng Z, Song W, Ma Z, Ma Y, Dang R, Zhang Z, Xu L, Jia Y, Liu S, Yue X, Deng W, Zhang X, Sun Z, Lan X, Han J, Chen H, Bradley DG, Jiang Y and Lei C, 2018. Whole-genome resequencing reveals world-wide ancestry and adaptive introgression events of domesticated cattle in East Asia. Nat Commun. 9(1):2337.

Cingolani P, Platts A, Wang LL, Coon M, Nguyen T, Wang L, Land SJ, Lu X, Ruden DM, 2012. A program for annotating and predicting the effects of single

687 nucleotide polymorphisms, SnpEff: SNPs in the genome of Drosophila
688 melanogaster strain w1118; iso-2; iso-3. Fly (Austin). 6(2):80-92.
689 Colgan TJ, Arce AN, Gill RJ, Ramos Rodrigues A, Kanteh A, Duncan EJ, Li L,
690 Chittka L, Wurm Y 2022. Genomic Signatures of Recent Adaptation in a Wild
691 Bumblebee. Mol Biol Evol. 39(2):msab366.
692 Dabney J, Knapp M, Glocke I, Gansauge M-T, Weihmann A, Nickel B, Valdiosera C,
693 García N, Pääbo S, Arsuaga J-L, 2013. Complete mitochondrial genome
694 sequence of a Middle Pleistocene cave bear reconstructed from ultrashort DNA
695 fragments. Proc. Natl. Acad. Sci. USA. 110(39):15758-15763.
696 Danecek P, Auton A, Abecasis G, Albers CA, Banks E, Depristo MA, Handsaker RE,
697 Lunter G, Marth GT, Sherry ST, Mcvean G and Durbin R, 2011. The variant call
698 format and VCFtools. Bioinformatics. 27(15):2156-2158.
699 Estoup A, Solignac M, Cornuet JM, Goudet J, Scholl A, 1996. Genetic differentiation
700 of continental and island populations of *Bombus terrestris* (Hymenoptera:
701 Apidae) in Europe. Molecular Ecology. 5(1):19-31.
702 Flousek J, Telenský T, Hanzelka J, Reif J, 2015. Population trends of central european
703 montane birds provide evidence for adverse impacts of climate change on
704 high-altitude species. PLoS One. 10(10):e0139465.
705 Fontaine C, Dajoz, I, Meriguet J, Loreau M, 2005. Functional diversity of
706 plant–pollinator interaction webs enhances the persistence of plant communities.
707 PLoS Biology. 4(1), e1.
708 Franks S, Hoffmann A, 2012. Genetics of climate change adaptation. Annu Rev Genet.
709 46:185-208.
710 Fuse N, 2017. Genome research elucidating environmental adaptation: Dark-fly
711 project as a case study. Curr Opin Genet Dev. 45(97-102).
712 Garibaldi L, Steffan-Dewenter I, Winfree R, Aizen M, Bommarco R, Cunningham S,
713 Klein A, 2013. Wild pollinators enhance fruit set of crops regardless of honey
714 bee abundance. Science. 339(6127): 1608-1611.
715 Goulson D, 2010. Impacts of non-native bumblebees in Western Europe and North
716 America. Applied Entomology and Zoology, 45(1):7-12.

717 Goulson D, Lye G, Darvill B, 2008. Decline and conservation of bumble bees. Annual
718 Review of Entomology. 53(1):191-208.
719 Goulson D, Nicholls E, Botías C, Rotheray E, 2015. Bee declines driven by combined
720 stress from parasites, pesticides, and lack of flowers. Science.
721 347(6229):1255957.
722 Grigory S, Potapov, Yulia S, Kolosova, 2016. Fauna of bumblebees (Hymenoptera:
723 Apidae: *Bombus Latreille*) in the mainland part of Arkhangelsk Region, NW
724 Russia, Annales de la Société entomologique de France (N.S.). 52:(3):150-160.
725 Halbritter A, Fior S, Keller I, Billeter R, Edwards PJ, Holderegger R, Karrenberg S,
726 Pluess AR, Widmer A, Alexander JM, 2018. Trait differentiation and adaptation
727 of plants along elevation gradients. J Evol Biol. 31(6):784-800.
728 Han E, Bauce É, 1995. Non-freeze survival of spruce budworm larvae, Choristoneura
729 fumiferana, at sub-zero temperatures during diapause. Entomologia
730 Experimentalis et Applicata. 75.
731 Hebert P, Penton E, Burns J, Janzen D, Hallwachs W, 2004. Ten species in one: DNA
732 barcoding reveals cryptic species in the neotropical skipper butterfly Astraptes
733 fulgerator. Proc Natl Acad Sci U S A. 101(41):14812-14817.
734 Heinrich B, 1974. Thermoregulation in endothermic insects. Science.
735 185(4153):747-56.
736 Hoffmann A, Sgrò C, 2011. Climate change and evolutionary adaptation. Nature.
737 470(7335):479-85.
738 Huang X, Kurata, N Wang, Z, Wang A, Zhao Q, Zhao Y, Guo Y, 2012. A map of rice
739 genome variation reveals the origin of cultivated rice. Nature.
740 490(7421):497-501.
741 Jones P, Binns D, Chang HY, Fraser M, Li W, McAnulla C, McWilliam H, Maslen J,
742 Mitchell A, Nuka G, Pesseat S, Quinn AF, Sangrador-Vegas A, Scheremetjew M,
743 Yong SY, Lopez R, Hunter S, 2014. InterProScan 5: genome-scale protein
744 function classification. Bioinformatics. 30(9):1236-1240.
745 Kerr J, Pindar A, Galpern P, Packer L, Potts SG, Roberts SM, Rasmont P, Schweiger
746 O, Colla SR, Richardson LL, Wagner DL, Gall LF, Sikes DS, Pantoja A, 2015.

CLIMATE CHANGE. Climate change impacts on bumblebees converge across continents. Science. 349(6244):177-80.

Kiełtyk P, 2021. Intraspecific morphological variation of Bellidiastrum michelii (Asteraceae) along a 1,155m elevation gradient in the Tatra Mountains. PeerJ. 9:e11286.

Koch J, Lozier J, Strange J, Ikerd H, Griswold T, Cordes N, Solter L, Stewart I and Cameron SA, 2015. USBombus, a database of contemporary survey data for north american bumble bees (Hymenoptera, Apidae, *Bombus*) distributed in the United States. Biodivers Data J 3(3):e6833.

Kraus FB, Wolf S, Moritz RF, 2009. Male flight distance and population substructure in the bumblebee *Bombus terrestris*. J Anim Ecol. 78(1):247-52.

Lecocq T, Vereecken NJ, Michez D, Dellicour S, Lhomme P, Valterová I, Rasplus JY, Rasmont P, 2013. Patterns of genetic and reproductive traits differentiation in Mainland vs. Corsican populations of bumblebees. PLoS One. 8(6):e65642.

Li H, Durbin R, 2009. Fast and accurate short read alignment with Burrows–Wheeler transform. Bioinformatics. 25(14):1754-1760.

Li H, Durbin R, 2011. Inference of human population history from individual whole-genome sequences. Nature. 475(7357):493-496.

Li H, Handsaker B, Wysoker A, Fennell T, Ruan J, Homer N, Marth G, Abecasis G, Durbin R, 2009. The sequence alignment/map format and SAMtools. Bioinformatics. 25(16):2078-2079.

Liu H, Jia Y, Sun X, Tian D, Hurst L, Yang S, 2017. Direct determination of the mutation rate in the bumblebee reveals evidence for weak recombination-associated mutation and an approximate rate constancy in insects. Mol Biol Evol. 34(1):119-130.

Liu X, Sun L., Xie Z, Yin X, Zhu R, Wang Y, 2007. A preliminary record of the historical seabird population in the Larsemann Hills, East Antarctica, from geochemical analyses of Mochou Lake sediments. Boreas. 36.

Lombardo JA, Elkinton JS, 2017. Environmental adaptation in an asexual invasive insect. Ecol Evol. 7(14):5123-5130.

Manichaikul A, Mychaleckyj JC, Rich SS, Daly K, Sale M, Chen W-M, 2010. Robust relationship inference in genome-wide association studies. Bioinformatics. 26(22):2867-2873.

Martin C, Fountain M, Brown M, 2019. Varietal and seasonal differences in the effects of commercial bumblebees on fruit quality in strawberry crops. Agric Ecosyst Environ. 281:124-133.

Marygold SJ, Crosby MA, Goodman JL, 2016. Using FlyBase, a database of Drosophila genes and genomes. Methods Mol. Biol. 1478:1-31.

McKenna A, Hanna M, Banks E, Sivachenko A, Cibulskis K, Kernytsky A, Garimella K, Altshuler D, Gabriel S, Daly M, 2010. The Genome Analysis Toolkit: a MapReduce framework for analyzing next-generation DNA sequencing data. Genome Res. 20(9):1297-1303.

Moreira A, Horgan F, Murray T, Kakouli-Duarte T, 2015. Population genetic structure of *Bombus terrestris* in Europe: Isolation and genetic differentiation of Irish and British populations. Molecular Ecology. 24(13):3257-3268.

Nasei J, Moinard C, Moreau L, Himpens B, Guyonnaud S, 1998. Relationship between aging, mating and sperm production in captive *Bombus terrestris*. J. Apic. Res. 37(2):107-113.

Patterson N, Price AL, Reich D, 2006. Population structure and eigenanalysis. PLoS Genet. 2(12).

Pavlidis P, Živkovic D, Stamatakis A, Alachiotis N, 2013. SweeD: likelihood-based detection of selective sweeps in thousands of genomes. Mol Biol Evol 30(9):2224-2234.

Pickrell JK, Pritchard JK, 2012. Inference of population splits and mixtures from genome-wide allele frequency data. PLoS Genet. 8(11):e1002967.

Potts S, Biesmeijer J, Kremen C, Neumann P, Schweiger O and Kunin W, 2010. Global pollinator declines: trends, impacts and drivers. Trends Ecol Evol. 25(6):345-53.

Qiu Q, Wang L, Wang K, Yang Y, Ma T, Wang Z, Zhang X, Ni Z, Hou F and Long R, 2015. Yak whole-genome resequencing reveals domestication signatures and

prehistoric population expansions. Nat Commun. 6(1):1-7.

Quinlan AR, Hall IM, 2010. BEDTools: a flexible suite of utilities for comparing genomic features. Bioinformatics. 26(6):841-842.

Rasmont P, Copp E, Michez D, Meulemeester T, 2008. An overview of the *Bombus terrestris* (L. 1758) subspecies (Hymenoptera: Apidae). Annales De La Socit Entomologique De France. 44(1):243-250.

Renault D, Salin C, Vannier G, Vernon P, 2002. Survival at low temperatures in insects: what is the ecological significance of the supercooling point? Cryo Letters. 23(4):217-28.

Rubin C, Megens H, Barrio A, Maqbool K, Sayyab S, Schwochow D, Wang C, Carlborg Ö, Jern P, Jørgensen C, 2012. Strong signatures of selection in the domestic pig genome. Proc Natl Acad Sci U S A. 109(48):19529-19536.

Sadd BM, Barribeau SM, Bloch G, et al, 2015 The genomes of two key bumblebee species with primitive eusocial organization. Genome Biol. 16(1):76.

Sang H, Li Y, Tan S, Gao P, Wang B, Guo S, Luo S, Sun C,2024. Conservation genomics analysis reveals recent population decline and possible causes in bumblebee *Bombus opulentus*. Insect Sci. PMID: 38297451..

Savolainen O, Lascoux M, Merilä J, 2013. Ecological genomics of local adaptation. Nat Rev Genet. 14(11):807-20.

Schmid-Hempel R, Schmid-Hempel P, 2000. Female mating frequencies in *Bombus* spp. from Central Europe. Insectes Soc. 47(1):36-41.

Silva S, Seabra S, Carvalheiro L, Nunes V, Marabuto E, Mendes R, Rodrigues A, Pina-Martins F, Yurtsever S, Laurentino T, 2020. Population genomics of *Bombus terrestris* reveals high but unstructured genetic diversity in a potential glacial refugium. Biol J Linn Soc. 129(2):259-272.

Smith B, Gehara M, Harvey M, 2021. The demography of extinction in eastern North American birds. Proc R Soc B. 288(1944).

Soroye P, Newbold T, Kerr J, 2020. Climate change contributes to widespread declines among bumble bees across continents. Science. 367(6478):685-688.

Spitze K, 1993. Population structure in Daphnia obtusa: quantitative genetic and

allozymic variation. Genetics. 135(2):367-374.

Stamatakis A, 2014. RAxML version 8: a tool for phylogenetic analysis and post-analysis of large phylogenies. Bioinformatics. 30(9):1312-3.

Sun C, Huang J, Wang Y, Zhao X, Su L, Thomas GWC, Zhao M, Zhang X, Jungreis I, Kellis M, Vicario S, Sharakhov IV, Bondarenko SM, Hasselmann M, Kim CN, Paten B, Penso-Dolfin L, Wang L, Chang Y, Gao Q, Ma L, Ma L, Zhang Z, Zhang H, Zhang H, Ruzzante L, Robertson HM, Zhu Y, Liu Y, Yang H, Ding L, Wang Q, Ma D, Xu W, Liang C, Itgen MW, Mee L, Cao G, Zhang Z, Sadd BM, Hahn MW, Schaack S, Barribeau SM, Williams PH, Waterhouse RM, Mueller RL, 2021. Genus-wide characterization of bumblebee genomes provides insights into their evolution and variation in ecological and behavioral traits. Mol Biol Evol. 38(2):486-501.

Sun Y, An Z, 2005. Late Pliocene-Pleistocene changes in mass accumulation rates of eolian deposits on the central Chinese Loess Plateau. J Geophys Res. 110(D23):D23101.

Tiusanen M, Huotari T, Hebert P, Andersson T, Asmus A, Bêty J, Davis E, Gale J, Hardwick B, Hik D, Körner C, Lanctot R, Loonen M, Partanen R, Reischke K, Saalfeld S, Senez-Gagnon F, Smith P, Šulavík J, Syvänperä I, Urbanowicz C, Williams S, Woodard P, Zaika Y, Roslin T, 2018. Flower-visitor communities of an arcto-alpine plant-Global patterns in species richness, phylogenetic diversity and ecological functioning. Molecular Ecology. 28:318-335.

Velthuis H, van Doorn A, 2006. A century of advances in bumblebee domestication and the economic and environmental aspects of its commercialization for pollination. Apidologie. 37(4):421-451.

Wang K, Li M, Hakonarson H, 2010. ANNOVAR: functional annotation of genetic variants from high-throughput sequencing data. Nucleic Acids Res. 38(16).

Williams PH, Cameron SA, Hines HM, Cederberg B, Rasmont P, 2008a. A simplified subgeneric classification of the bumblebees (genus *Bombus*). Apidologie. 39(1):46-74.

Williams P, Lobo J, Meseguer A, 2018. Bumblebees take the high road: climatically

integrative biogeography shows that escape from Tibet, not Tibetan uplift, is associated with divergences of present-day Mendacibombus. Ecography. 41(3):461-477.

Williams S, Shoo L, Isaac J, Hoffmann A, Langham G, Mathur H, 2008. Towards an integrated framework for assessing the vulnerability of species to climate change. PLoS Biol. 6:e325.

Xia Q, Guo Y, Zhang Z, Li D, Xuan Z, Li Z, Dai F, Li Y, Cheng D, Li R, Cheng T, Jiang T, Becquet C, Xu X, Liu C, Zha X, Fan W, Lin Y, Shen Y, Jiang L, Jensen J, Hellmann I, Tang S, Zhao P, Xu H, Yu C, Zhang G, Li J, Cao J, Liu S, He N, Zhou Y, Liu H, Zhao J, Ye C, Du Z, Pan G, Zhao A, Shao H, Zeng W, Wu P, Li C, Pan M, Li J, Yin X, Li D, Wang J, Zheng H, Wang W, Zhang X, Li S, Yang H, Lu C, Nielsen R, Zhou Z, Wang J, Xiang Z, Wang J, 2009. Complete resequencing of 40 genomes reveals domestication events and genes in silkworm (Bombyx). Science. 326(5951):433-436.

Xie C, Mao X, Huang J, Ding Y, Wu J, Dong S, Kong L, Gao G, Li CY, Wei L, 2011. KOBAS 2.0: a web server for annotation and identification of enriched pathways and diseases. Nucleic Acids Res. 39.

Zhao G, Lian Q, Zhang Z, Fu Q, He Y, Ma S, Ruggieri V, Monforte AJ, Wang P, Julca I, 2019. A comprehensive genome variation map of melon identifies multiple domestication events and loci influencing agronomic traits. Nat Genet. 51(11):1607-1615.

Zhao S, Zheng P, Dong S, Zhan X, Wu Q, Guo X, Hu Y, He W, Zhang S, Fan W, Zhu L, Li D, Zhang X, Chen Q, Zhang H, Zhang Z, Jin X, Zhang J, Yang H, Wang J, Wang J, Wei F, 2013. Whole-genome sequencing of giant pandas provides insights into demographic history and local adaptation. Nat Genet. 45(1):67-71.

Zheng B, Xu Q, Shen Y, 2002. The relationship between climate change and Quaternary glacial cycles on the Qinghai–Tibetan Plateau: review and speculation. Quaternary International, 97(98):93-101.

Zhou X, Wang B, Pan Q, Zhang J, Kumar S, Sun X, Liu Z, Pan H, Lin Y, Liu G, 2014. Whole-genome sequencing of the snub-nosed monkey provides insights into

897 folivory and evolutionary history. Nat Genet. 46(12):1303-1310.
898 Zhou Z, Jiang Y, Wang Z, Gou Z, Lyu J, Li W, Yu Y, Shu L, Zhao Y, Ma Y, Fang C,
899 Shen Y, Liu T, Li C, Li Q, Wu M, Wang M, Wu Y, Dong Y, Wan W, Wang X,
900 Ding Z, Gao Y, Xiang H, Zhu B, Lee SH, Wang W, Tian Z, 2015. Resequencing
901 302 wild and cultivated accessions identifies genes related to domestication and
902 improvement in soybean. Nat Biotechnol. 33(4):408-414.
903 Zhu Y, Siegwolf RT, Durka W, Körner C, 2010. Phylogenetically balanced evidence
904 for structural and carbon isotope responses in plants along elevational gradients.
905 Oecologia. 162(4):853-63.
906

Supplementary Materials:

Table S1 Summary of wild samples information

Sample	Site_country	Site_province	Site_name	Collect_date	Longitude	Latitude
ALT1	China	Xinjiang	Altay	2019.6	88.1411°E	47.8522°N
ALT2	China	Xinjiang	Altay	2019.6	88.1411°E	47.8522°N
ALT3	China	Xinjiang	Altay	2019.6	88.1411°E	47.8522°N
ALT4	China	Xinjiang	Altay	2019.6	88.1411°E	47.8522°N
ALT5	China	Xinjiang	Altay	2019.6	88.1411°E	47.8522°N
ALT6	China	Xinjiang	Buerjin	2018.6	86.52°E	47.42°N
ALT7	China	Xinjiang	Buerjin	2018.6	86.52°E	47.42°N
BEJ1	China	Xinjiang	Buerjin	2019.6	86.52°E	47.42°N
BEJ2	China	Xinjiang	Buerjin	2019.6	86.52°E	47.42°N
BEJ3	China	Xinjiang	Buerjin	2019.6	86.52°E	47.42°N
BEJ4	China	Xinjiang	Buerjin	2019.6	86.52°E	47.42°N
BEJ5	China	Xinjiang	Buerjin	2019.6	86.52°E	47.42°N
BEJ6	China	Xinjiang	Buerjin	2018.6	86.52°E	47.42°N
EM1	China	Xinjiang	Emin	2019.6	83.6133°E	46.5238°N
EM2	China	Xinjiang	Emin	2019.6	83.6133°E	46.5238°N
EM3	China	Xinjiang	Emin	2019.6	83.6133°E	46.5238°N
EM4	China	Xinjiang	Emin	2019.6	83.6133°E	46.5238°N
FY1-1	China	Xinjiang	Fuyun	2019.6	89.535°E	46.9811°N
FY1-2	China	Xinjiang	Fuyun	2019.6	89.535°E	46.9811°N
FY1-3	China	Xinjiang	Fuyun	2019.6	89.535°E	46.9811°N
FY1-4	China	Xinjiang	Fuyun	2019.6	89.535°E	46.9811°N
FY1-5	China	Xinjiang	Fuyun	2019.6	89.535°E	46.9811°N
FY2-1	China	Xinjiang	Fuyun	2019.6	89.8233°E	47.2141°N
FY2-2	China	Xinjiang	Fuyun	2019.6	89.8233°E	47.2141°N
FY2-3	China	Xinjiang	Fuyun	2019.6	89.8233°E	47.2141°N
FY2-4	China	Xinjiang	Fuyun	2019.6	89.8233°E	47.2141°N
FY2-5	China	Xinjiang	Fuyun	2019.6	89.8233°E	47.2141°N
HEBU1	China	Xinjiang	Hoboksar	2019.6	85.7236°E	46.7869°N
HEBU2	China	Xinjiang	Hoboksar	2019.6	85.7236°E	46.7869°N
HEBU3	China	Xinjiang	Hoboksar	2019.6	85.7236°E	46.7869°N
JMN1	China	Xinjiang	Jimunai	2019.6	85.8697°E	47.4169°N
JMN2	China	Xinjiang	Jimunai	2019.6	85.8697°E	47.4169°N
JMN3	China	Xinjiang	Jimunai	2019.6	85.8697°E	47.4169°N
JMN4	China	Xinjiang	Jimunai	2019.6	85.8697°E	47.4169°N
TC1	China	Xinjiang	Tacheng	2018.6	82.5189°E	45.9499°N
TC2	China	Xinjiang	Tacheng	2018.6	82.5189°E	45.9499°N
TGG1	China	Xinjiang	Tiechanggou	2019.6	84.4494°E	46.1672°N
TGG2	China	Xinjiang	Tiechanggou	2019.6	84.4494°E	46.1672°N
TGG3	China	Xinjiang	Tiechanggou	2019.6	84.4494°E	46.1672°N
TGG4	China	Xinjiang	Tiechanggou	2019.6	84.4494°E	46.1672°N

TGG5	China	Xinjiang	Tiechanggou	2019.6	84.4494°E	46.1672°N
Fra	France	Perpignan	Perpignan	2018.1	2.89541°E	42.6976°N
Ger	Germany	NR-Westfalia	Muenster	2011.4	6.953101°E	50.9351°N
Kyr	Kyrgyzstan	Issyk-Kul	Barskoon	2009.7	77.5°E	42.5°N
Rus	Russia	Novosibirsk	Chany lake	2006.5	82.9339°E	55.0188°N
Swe	Sweden	Uppsala	Predikstolen	2011.4	17.6388°E	59.8588°N
Swi1	Switzerland	Zuerich	Hedingen	2011.4	8.55°E	47.3667°N
Swi2	Switzerland	Graubuenden	San Bernardino	2011.4	9.54972°E	46.6497°N
Taj	Tajikistan	Kuhistoni Badakhshon	Shirg	2009.5	71.2715°E	38.3234°N
Tur1	Turkey	Sinop	Alaçam-Durağan	2010.5	35.1625°E	42.0268°N
Tur2	Turkey	Edirne	İbriktepe-Uzunköprü	2010.5	26.5834°E	41.6749°N
Tur3	Turkey	Samsun	Alaçam-Durağan	2010.5	36.3361°E	41.2797°N
UK	UK	England	Shortlands	2011.4	0.136439°W	51.5073°N

Table S2 Quality control data

Sample	Raw Base(bp)	Clean Base(bp)	Effective Rate(%)	Error Rate(%)	Q20(%)	Q30(%)	GC Content(%)
ALT1	11204490000	11187918300	99.85	0.03	97.72	94.06	39.61
ALT2	11115318900	11099028900	99.85	0.03	98.05	94.65	39.61
ALT3	11735084700	11717913300	99.85	0.03	98.01	94.37	39.6
ALT4	11775414600	11758554000	99.86	0.03	97.89	94.22	39.22
ALT5	11232938700	11214195900	99.83	0.03	97.48	93.5	40.71
ALT6	23198895000	22913028300	98.77	0.04	94.15	87.45	39.04
ALT7	23425786800	23162517900	98.88	0.04	94.81	88.52	38.56
BEJ1	18807973500	18740560200	99.64	0.03	96.41	91.58	38.34
BEJ2	15412268100	15361805100	99.67	0.03	96.11	90.62	38.13
BEJ3	17629497000	17567310000	99.65	0.03	96.66	91.97	38.23
BEJ4	14801996400	14752334400	99.66	0.03	96.57	91.67	38.25
BEJ5	18776677200	18711360000	99.65	0.03	96.13	91.13	38.92
BEJ6	23495247000	23403879600	99.61	0.03	96.25	91.45	39.09
EM1	11361333600	11344302600	99.85	0.03	97.83	94.18	40.6
EM2	11335378500	11318334600	99.85	0.03	97.94	94.33	40.89
EM3	11329419600	11313071100	99.86	0.03	97.88	94.18	39.71
EM4	11083358100	11066329200	99.85	0.03	97.58	93.5	40.49
Fra	10276995564	10296814276	99.19	0.02	97.92	91.96	36.24
FY1_1	11684118900	11666343000	99.85	0.03	97.59	93.54	39.94
FY1_2	11458690500	11441256000	99.85	0.03	97.69	93.86	39.81
FY1_3	11383016100	11367117900	99.86	0.03	98.05	94.41	39.19
FY1_4	11297316300	11280502200	99.85	0.03	97.9	94.1	39.99
FY1_5	11012565600	10996983000	99.86	0.03	98.17	94.65	39.01
FY2_1	11535843300	11518626300	99.85	0.03	97.84	94	39.84
FY2_2	11772026100	11755001700	99.86	0.03	97.98	94.43	39.51

FY2_3	11252029200	11235295500	99.85	0.03	97.96	94.17	39.46
FY2_4	11187132600	11170856100	99.85	0.03	98.14	94.57	39.43
FY2_5	11267707200	11251611000	99.86	0.03	98.08	94.37	39.07
Ger	19210869156	19259124154	99.25	0.02	99.16	94.04	36.89
HEBU_1	11825811300	11807268900	99.84	0.03	97.61	93.84	40.51
HEBU_2	11267631600	11250558600	99.85	0.03	97.68	93.88	40.19
HEBU_3	11960218800	11942794200	99.85	0.03	97.9	94.34	39.94
JMN1	11800650000	11782890900	99.85	0.03	97.6	93.77	39.76
JMN2	11720851800	11702907000	99.85	0.03	97.44	93.11	40.29
JMN3	11955773400	11937270000	99.85	0.03	97.58	93.41	40.56
JMN4	11885277900	11867463300	99.85	0.03	97.67	93.81	40.03
KA1	21588184200	21485203500	99.52	0.03	95.92	90.17	37.87
KA2	11280674700	11264512800	99.86	0.03	97.42	93.13	39.98
KA3	11446620600	11430573300	99.86	0.03	97.45	93.22	39.85
KB1	11750325000	11732830200	99.85	0.03	97.42	93.22	41.18
KB2	11186355600	11170710600	99.86	0.03	97.51	93.16	40.15
KB3	14625807300	14542490700	99.43	0.04	95.74	89.97	37.69
KC1	11661643500	11645530800	99.86	0.03	97.72	93.55	39.65
KC2	14553318900	14468098800	99.41	0.03	95.87	90.24	37.85
KD1	14658367800	14577426600	99.45	0.03	96.26	91.03	37.68
KD2	11394051900	11377847400	99.86	0.03	97.34	93.02	40.18
KE1	10455830700	10441926000	99.87	0.03	97.73	93.47	39.48
KE2	22805772900	22611616800	99.15	0.04	94.14	87.2	38.63
KF1	10703553900	10688679000	99.86	0.03	97.78	93.56	39.55
KF2	13262647200	13177446000	99.36	0.03	95.97	90.64	37.66
Kyr	8945049448	8979111710	99.38	0.03	97.14	89.88	42.57
Rus	9143354894	9174609276	99.34	0.02	98.5	92.42	38.3
Swe	13788343410	13842519176	99.39	0.02	98.79	92.79	39.98
Swi1	13300134086	13364984922	99.49	0.03	97.61	90.2	40.51
Swi2	13926376400	13974411124	99.34	0.02	99.31	93.93	37.55
Taj	11782210764	11824882844	99.36	0.02	99.12	93.64	36.36
TC1	19229094600	19163923500	99.66	0.03	96.02	90.53	38.41
TC2	18362369400	18298855200	99.65	0.03	96.57	91.69	38.43
TGG1	11160099300	11142984300	99.85	0.03	97.71	93.7	40.04
TGG2	11674034700	11655866400	99.84	0.03	97.37	93.02	40.53
TGG3	11958380700	11940497700	99.85	0.03	97.56	93.4	39.48
TGG4	11868649200	11850252300	99.84	0.03	97.27	93.01	39.9
TGG5	11084604600	11067224700	99.84	0.03	97.78	94.04	40.24
Tur1	22865317378	22920106310	99.24	0.02	98.34	92.9	36.99
Tur2	13949746442	13987439470	99.27	0.02	98.76	93.33	37.53
Tur3	8935426978	8984988552	99.55	0.02	99.54	93.36	39.21
UK	18842955980	18903012926	99.32	0.02	99.89	94.82	36.76

Table S3 Resequencing Mapping data

Sample	Total reads	Mapping rate(%)	Total mapped reads	Multiple mapped reads	Uniquely mapped reads	Read-1	Read-2	Reads map to '+'	Reads map to '-'	Reads mapped in proper pairs	Proper-paired reads map to different chrom	Average depth(X)	Coverage_at_least_1X(%)	Coverage_at_least_4X(%)
ALT1	60338531	93.36	56334946	8585893	47749053	23927372	23821681	23759724	23989329	43420049	9763	30.89	99.46	98.86
ALT2	59654151	95.39	56909122	6995849	49913273	25008832	24904441	24855850	25057423	46539085	7669	32.36	99.47	98.85
ALT3	63611199	95.66	60856358	6328997	54527361	27320237	27207124	27186368	27340993	51110639	7206	35.36	99.44	98.76
ALT4	63013055	95.28	60039969	7624607	52415362	26264906	26150456	26105064	26310298	48740347	7421	34.02	99.46	98.89
ALT5	60992306	95.28	58113625	7293087	50820538	25475301	25345237	25281758	25538780	47181846	6297	32.71	99.26	97.97
ALT6	119996576	93.92	112705201	19452529	93252672	46791149	46461523	46335951	46916721	86174678	10352	58.43	99.56	99.46
ALT7	123119603	93.09	114615431	17767522	96847909	48538308	48309601	48163402	48684507	90131000	8143	60.77	99.56	99.47
BEJ1	95133567	94.01	89443397	18571438	70871959	35524235	35347724	35129475	35742484	63251595	19123	44.7	99.6	99.48
BEJ2	80892647	94.05	76085398	14708434	61376964	30793897	30583067	30485216	30891748	55170151	11547	39.18	99.58	99.45
BEJ3	90418240	94.57	85511905	16700707	68811198	34501876	34309322	34155166	34656032	61535487	16335	43.54	99.59	99.47
BEJ4	77542745	94.98	73653368	15784769	57868599	29025466	28843133	28701654	29166945	51444292	14737	36.89	99.57	99.41
BEJ5	95346283	94.86	90450616	19323838	71126778	35658659	35468119	35251475	35875303	63519076	17431	44.88	99.56	99.35
BEJ6	117565589	94.65	111284123	25191796	86092327	43148822	42943505	42631059	43461268	75823171	27232	53.51	99.57	99.38
EM1	61495421	91.54	56293020	6745208	49547812	24828220	24719592	24671246	24876566	45969444	6968	31.88	99.42	98.63
EM2	61895265	85.82	53120224	6230533	46889691	23496010	23393681	23351911	23537780	43683586	6632	30.31	99.44	98.79
EM3	60727176	93.89	57016852	7883251	49133601	24617674	24515927	24455621	24677980	45124738	7815	31.63	99.49	98.97
EM4	60394566	95.23	57519590	6535415	50984175	25552479	25431696	25396990	25587185	47432540	4903	32.79	99.38	98.46
Fra	49084411	94.73	46500676	20032178	26468498	13297046	13171452	12784761	13683737	21313403	35476	16.74	99.15	89.04
FY1_1	63452384	94.48	59952206	7723265	52228941	26175399	26053542	25997062	26231879	48532552	7985	33.76	99.37	98.49
FY1_2	63741273	92.9	59217390	7398523	51818867	25964147	25854720	25804893	26013974	47964603	6712	33.36	99.41	98.62
FY1_3	62252460	91.1	56716482	5704712	51011770	25558343	25453427	25439282	25572488	48052887	5722	33.22	99.4	98.64
FY1_4	62231623	94.68	58926659	5693775	53232884	26673630	26559254	26542337	26690547	50045797	4893	34.39	99.4	98.6

FY1_5	60205388	93.17	56098841	5611934	50486907	25292899	25194008	25183008	25303899	47462865	6031	32.84	99.52	99.02
FY2_1	64056196	94.69	60654861	5728628	54926233	27521477	27404756	27390227	27536006	51779018	5721	35.47	99.46	98.87
FY2_2	61946045	94.93	58810019	7195089	51614930	25864108	25750822	25704464	25910466	47925437	5874	33.32	99.49	99.07
FY2_3	62475568	94.31	58924095	5396677	53527418	26820347	26707071	26703016	26824402	50458453	4684	34.63	99.48	98.96
FY2_4	61729408	95.79	59131187	5156064	53975123	27039518	26935605	26942401	27032722	51052354	5329	35.05	99.48	98.98
FY2_5	61170084	95.4	58359605	4534160	53825445	26969141	26856304	26873546	26951899	50956687	4371	34.91	99.49	99.04
Ger	89444971	94.82	84811909	28783251	56028658	28164296	27864362	27138255	28890403	48299394	43890	33.74	99.54	99.4
HEBU_1	62547965	94.95	59392812	8634481	50758331	25433825	25324506	25223819	25534512	46702021	7938	32.51	99.37	98.42
HEBU_2	60455961	95.08	57483570	7687860	49795710	24952770	24842940	24780493	25015217	46075073	7640	32.1	99.36	98.41
HEBU_3	63374407	94.85	60112866	8494592	51618274	25863748	25754526	25677838	25940436	47613575	9090	33.4	99.37	98.49
JMN1	63643992	93.41	59453158	9410416	50042742	25076478	24966264	24894358	25148384	45303754	12938	32.31	99.42	98.67
JMN2	64176692	94.72	60792789	7081620	53711169	26924088	26787081	26756485	26954684	49883611	7118	34.65	99.38	98.52
JMN3	66461312	93.32	62027276	5952415	56074861	28104715	27970146	27960672	28114189	52349473	5818	36.08	99.39	98.56
JMN4	63577381	94.29	59951240	9018400	50932840	25523762	25409078	25339162	25593678	46550748	8549	32.86	99.42	98.61
KA1	113388951	93.33	105827064	21175744	84651320	42535101	42116219	42074528	42576792	75728118	24550	54.04	99.58	99.45
KA2	59036920	93.65	55290621	9696785	45593836	22847309	22746527	22663907	22929929	41258919	11920	29.39	99.46	98.78
KA3	60953643	93.93	57258068	10215513	47042555	23577590	23464965	23388587	23653968	42452721	9864	30.38	99.43	98.67
KB1	60455341	93.37	56452788	9836690	46616098	23363930	23252168	23134263	23481835	42234693	7322	29.7	99.26	97.73
KB2	58652809	94.6	55486572	8959711	46526861	23314403	23212458	23123829	23403032	42650958	8102	30.05	99.35	98.31
KB3	82680237	94.52	78154868	16615803	61539065	30940793	30598272	30582371	30956694	54806123	22609	39.63	99.55	99.28
KC1	61276422	94.98	58203780	8798498	49405282	24755108	24650174	24586273	24819009	45503983	8652	32.04	99.44	98.73
KC2	82360268	94.03	77448058	17266359	60181699	30245179	29936520	29897223	30284476	53299067	25226	38.77	99.53	99.21
KD1	79621366	94.56	75290434	17330808	57959626	29108140	28851486	28765792	29193834	51284318	33024	37.21	99.53	99.21
KD2	59916818	93.6	56087621	10978459	45109162	22613442	22495720	22396234	22712928	40307179	9561	28.94	99.37	98.31
KE1	55309885	95.19	52650072	9001986	43648086	21875298	21772788	21694802	21953284	39861045	12424	28.35	99.34	98.25
KE2	119039176	94.39	112361656	20815446	91546210	46067497	45478713	45463709	46082501	84205906	11416	57.11	99.56	99.47
KF1	57970580	95.18	55178787	7160589	48018198	24057731	23960467	23924642	24093556	44820919	6845	31.28	99.41	98.66

KF2	72410422	94.21	68220227	16143414	52076813	26154009	25922804	25857045	26219768	45839907	32358	33.57	99.52	99.09
Kyr	36328608	92.08	33452400	15453978	17998422	9067289	8931133	8374828	9623594	14205919	16508	11.3	96.9	62.62
Rus	40670848	91.81	37342707	15558931	21783776	10954711	10829065	10395816	11387960	17876497	17809	13.6	98.38	77.69
Swe	60097130	94.28	56664413	20929970	35734443	17983724	17750719	17078532	18655911	30480001	35358	21.72	99.48	97.82
Swi1	54370698	94.16	51199877	24019919	27179958	13658897	13521061	12584321	14595637	21721470	35970	16.11	98.9	83.62
Swi2	62075585	93.96	58331677	23273660	35058017	17645813	17412204	16811128	18246889	29225829	48406	21.11	99.43	96.14
Taj	51792271	94.69	49042231	20308877	28733354	14478209	14255145	13646535	15086819	23853377	26584	17.4	99.2	90.91
TC1	99412970	94.93	94380746	19968379	74412367	37372430	37039937	36883138	37529229	66022449	20288	47.15	99.57	99.39
TC2	95977691	94.97	91153502	18333177	72820325	36519368	36300957	36129695	36690630	65257177	20195	46.36	99.57	99.37
TGG1	61855671	94.75	58613219	5899442	52713777	26417381	26296396	26275993	26437784	49477581	6540	34.05	99.41	98.65
TGG2	64094359	94.66	60672737	7363286	53309451	26723633	26585818	26549008	26760443	49300945	6017	34.24	99.44	98.74
TGG3	65867463	94.46	62219334	7486047	54733287	27429503	27303784	27267648	27465639	50834835	7173	35.38	99.51	99.1
TGG4	64500247	93.77	60484029	9023049	51460980	25798388	25662592	25586483	25874497	47003214	11237	33.02	99.48	98.93
TGG5	60824481	94.8	57662685	6145779	51516906	25814670	25702236	25668215	25848691	48139251	5544	33.21	99.42	98.66
Tur1	98790062	94.85	93707616	39919147	53788469	27082405	26706064	26065515	27722954	42146079	63734	32.14	99.53	99.22
Tur2	62243048	94.68	58931758	22424925	36506833	18355068	18151765	17546130	18960703	30730479	41716	22.6	99.47	97.63
Tur3	37487108	94.47	35417741	14879172	20538569	10330428	10208141	9692036	10846533	17455686	20243	12.87	97.79	72.39
UK	92884998	85.13	79077626	24320759	54756867	27499353	27257514	26608404	28148463	48142955	41538	32.58	99.53	99.39

Table S4 Morphological parameters of *Bombus terrestris* from Asia and Europe

Samples	Proboscis length (mm)	Forewing length (FL) (mm)	Forewing width (FB) (mm)	Cubital vein A (mm)	Cubital vein B (mm)	Wing vein angles (A4)	Hooks on the right HW	Femur length (Fe) (mm)	Tibia length (Ti)	Metabasitarsus length (ML)	Metabasitarsus width (MT)	Length of the third AS(S3)	Width of the third AS	Width of the fourth AS	Length of the genitalia	Width of the genitalia.
Quene1 (Europe)	10.4112	17.5398	6.1315	1.2163	0.2613	63.06	27	5.408	6.1214	3.9449	1.6187	4.1814	4.1873	4.2405	Ne	Ne
Quene2 (Europe)	9.7037	18.4261	6.2687	1.3142	0.4067	58.83	25	6.0861	6.6174	4.4188	1.7232	4.5342	4.1	4.2082	Ne	Ne
Quene3 (Europe)	9.4724	19.012	6.7831	1.3509	0.3245	56.84	24	6.0872	6.6894	4.2735	1.6094	4.4417	4.3263	4.3592	Ne	Ne
Quene4 (Europe)	9.3975	19.2258	6.7599	1.3238	0.3188	62.95	23	6.1954	6.6988	4.2599	1.8474	4.435	4.2318	4.1464	Ne	Ne

Quene5 (Asia)	12.2255	18.386	6.6507	1.2868	0.3279	57.82	24	5.7862	6.3415	4.1448	1.498	4.3373	4.3719	4.5119	Ne	Ne
Quene6 (Asia)	11.903	20.163	6.4159	1.2875	0.3248	58.63	25	5.9702	6.737	4.2107	1.816	4.4916	4.7467	4.8806	Ne	Ne
Quene7 (Asia)	12.3177	Ne	Ne	1.3221	0.3343	54.27	21	5.7716	6.3946	3.8764	1.9231	4.52	4.4885	4.4555	Ne	Ne
Quene8 (Asia)	9.261	18.7405	6.8364	1.3043	0.3909	58.07	25	5.9044	6.4404	4.1114	1.5477	4.3748	4.4725	4.3322	Ne	Ne
Worker1 (Europe)	10.744	14.1841	4.7941	1.0905	0.2312	53.97	21	4.3827	5.0336	3.2887	1.493	3.0932	3.1311	2.9482	Ne	Ne
Worker2 (Europe)	9.3299	13.0988	4.4018	0.9649	0.2388	60.46	Ne	3.9379	4.6479	2.9845	1.2746	2.7784	3.0862	2.9391	Ne	Ne
Worker3 (Europe)	7.7166	13.6721	4.5599	0.9872	0.253	58.79	19	4.3218	4.9539	3.1981	1.0928	3.0426	2.9456	3.0823	Ne	Ne
Worker4 (Europe)	9.5424	13.3436	4.3631	1.0408	0.1762	60.15	19	4.3201	4.7934	2.9015	1.2235	2.7477	2.7637	2.6289	Ne	Ne
Worker5 (Europe)	8.4483	11.8039	3.8508	0.8391	0.2125	63.31	18	3.7221	4.2717	2.6943	1.1432	2.3505	2.6258	2.5748	Ne	Ne
Worker6 (Europe)	8.9773	11.5977	3.9044	0.8863	0.2	63.64	20	3.6239	4.0617	2.5299	0.9909	2.5878	2.6097	2.5397	Ne	Ne
Worker7 (Europe)	9.3698	12.4825	4.0306	0.957	0.237	64.9	Ne	3.8061	4.2899	2.5549	1.089	2.6259	2.6009	2.6748	Ne	Ne
Worker8 (Europe)	8.999	12.6347	4.2691	0.905	0.1834	61	Ne	3.8647	4.4682	2.504	1.1802	2.6624	2.5652	2.5438	Ne	Ne
Worker9 (Asia)	5.8474	14.2056	4.8861	0.9756	0.2394	67.74	22	4.2199	4.8215	3.1507	1.11	2.971	2.8967	2.8497	Ne	Ne
Worker10 (Asia)	9.4011	13.8672	4.6852	1.0198	0.2114	59.96	19	4.093	4.7017	2.8332	1.0694	2.6879	2.8698	2.8635	Ne	Ne
Worker11 (Asia)	7.3736	13.9833	5.0537	1.0595	0.2226	62.85	21	4.5194	5.1186	3.2558	1.3205	3.051	3.0376	3.0521	Ne	Ne
Worker12 (Asia)	6.8042	13.2847	4.597	0.9294	0.2041	68.2	19	3.7457	4.6828	2.9038	1.2733	2.8457	2.9032	2.8246	Ne	Ne
Worker13 (Asia)	7.0999	13.1033	4.4682	0.9657	0.1621	59.99	20	4.0005	4.5332	3.0164	1.0858	2.5261	2.7674	2.6413	Ne	Ne
Worker14 (Asia)	6.4625	13.0296	4.5497	0.9844	0.1931	66.82	21	4.1587	4.4164	2.7043	1.1838	2.7408	2.8501	2.7304	Ne	Ne
Worker15 (Asia)	5.8337	11.7578	4.1724	0.8779	0.1661	66.3	Ne	3.6425	4.2671	2.4462	1.0944	2.5718	2.6077	2.5947	Ne	Ne
Worker16 (Asia)	5.592	11.5655	4.0893	0.8509	0.149	64.9	Ne	3.6911	4.1535	2.5098	1.1448	2.473	2.3379	2.5203	Ne	Ne
Drone1 (Europe)	10.2915	15.6712	5.2925	1.2625	0.2114	62.69	22	4.8895	5.4519	3.4057	1.0828	2.9812	3.1807	3.032	3.7611	3.1212
Drone2 (Europe)	9.9549	15.1592	5.1133	1.1808	0.2786	62.41	21	4.6737	5.2004	3.3021	1.1929	3.1356	3.1067	2.9153	3.634	2.9617
Drone3 (Europe)	9.3952	14.0753	4.6646	1.101	0.2385	63.71	21	3.9129	4.735	3.0184	1.106	2.6434	2.8166	2.633	3.7334	2.9031
Drone4 (Europe)	10.2598	16.2548	5.4413	1.1309	0.2414	59.44	20	4.5011	5.1793	3.3552	1.0641	3.2206	3.2839	3.0838	3.7811	3.0284
Drone5 (Europe)	9.283	14.363	4.725	1.1073	0.2313	65.07	18	4.4765	4.7765	3.1456	1.0391	2.4889	2.8802	2.6733	3.5177	2.835
Drone6 (Europe)	9.709	15.1516	5.3141	1.2353	0.2127	61.95	21	4.8731	5.3343	3.6161	1.0395	2.5528	3.0644	2.7639	3.6058	3.0253
Drone7 (Asia)	6.4657	14.2648	4.7417	1.1043	0.2169	67.51	19	4.4485	4.7471	3.0062	0.8887	2.8405	2.9933	2.5878	3.1018	2.5334
Drone8 (Asia)	6.5009	14.6338	5.0494	1.1197	0.2481	65.24	18	4.3929	4.7772	3.3388	0.9929	2.9571	2.9948	2.8565	3.1716	2.8098
Drone9 (Asia)	9.4718	15.3852	5.1741	1.1827	0.2293	60.83	21	4.8082	5.1491	3.5045	1.0605	2.8608	3.0123	2.9103	3.6724	3.1491
Drone10 (Asia)	9.3874	15.2316	5.064	1.0883	0.2698	64.12	20	4.5496	5.0908	3.4434	1.0504	2.7571	2.8808	2.6395	3.6813	3.0488
Drone11 (Asia)	9.3217	15.1639	5.232	1.1445	0.3029	63.73	20	4.477	5.0358	3.3787	1.0174	2.8574	3.0672	2.9133	3.304	3.0587
Drone12 (Asia)	8.6073	13.533	4.6486	1.0504	0.2615	66.18	19	3.9883	4.5594	3.1083	1.0469	2.5348	2.8323	2.706	3.4151	2.7568

Table S5 GO enrichment analysis of Asia samples selected genes

GO.ID	Term	Annotated	Selected	Expected	Fis p-value
GO:0007165	signal transduction	484	34	16.95	4.10E-05
GO:0007154	cell communication	496	34	17.37	6.80E-05
GO:0023052	signaling	498	34	17.44	7.40E-05
GO:0050789	regulation of biological process	994	55	34.81	0.00012
GO:0050794	regulation of cellular process	964	53	33.76	0.0002
GO:0050896	response to stimulus	644	39	22.56	0.00028
GO:0065007	biological regulation	1042	55	36.49	0.00043
GO:0051716	cellular response to stimulus	598	36	20.94	0.00057
GO:0043087	regulation of GTPase activity	17	4	0.6	0.00241
GO:0035556	intracellular signal transduction	193	15	6.76	0.00281
GO:0006487	protein N-linked glycosylation	4	2	0.14	0.00698
GO:0016477	cell migration	4	2	0.14	0.00698
GO:0051336	regulation of hydrolase activity	23	4	0.81	0.00762
GO:0007166	cell surface receptor signaling pathway	69	7	2.42	0.00985
GO:0007275	multicellular organism development	39	5	1.37	0.01087
GO:0006182	cGMP biosynthetic process	6	2	0.21	0.01666
GO:0007093	mitotic cell cycle checkpoint	6	2	0.21	0.01666
GO:0045930	negative regulation of mitotic cell cycl...	6	2	0.21	0.01666
GO:0046068	cGMP metabolic process	6	2	0.21	0.01666
GO:0048870	cell motility	6	2	0.21	0.01666
GO:0051674	localization of cell	6	2	0.21	0.01666
GO:0016051	carbohydrate biosynthetic process	16	3	0.56	0.01687
GO:0048856	anatomical structure development	46	5	1.61	0.02128
GO:0040011	locomotion	7	2	0.25	0.0228
GO:0051304	chromosome separation	8	2	0.28	0.0297
GO:0032502	developmental process	52	5	1.82	0.03417
GO:0043547	positive regulation of GTPase activity	9	2	0.32	0.03732
GO:0052652	cyclic purine nucleotide metabolic proce...	9	2	0.32	0.03732
GO:0007155	cell adhesion	38	4	1.33	0.04241
GO:0022610	biological adhesion	38	4	1.33	0.04241
GO:0009653	anatomical structure morphogenesis	10	2	0.35	0.0456
GO:0051345	positive regulation of hydrolase activit...	10	2	0.35	0.0456
GO:0048523	negative regulation of cellular process	57	5	2	0.04797

Table S6 KEGG enrichment analysis of Asia samples selected genes

KEGG Term	ID	Input number	Background number	P-Value
MAPK signaling pathway - fly	bter04013	10	82	3.73E-05
Wnt signaling pathway	bter04310	9	69	5.69E-05
Glycerophospholipid metabolism	bter00564	5	57	0.012256
Apoptosis - fly	bter04214	4	46	0.025026
Hippo signaling pathway - fly	bter04391	4	48	0.028428

Table S7 Asia samples selected genes

LOC100631093	LOC100642192	LOC100642226	LOC100642240	LOC100642243	LOC100642360
LOC100642364	LOC100642426	LOC100642441	LOC100642479	LOC100642485	LOC100642559
LOC100642587	LOC100642596	LOC100642681	LOC100642697	LOC100642792	LOC100642813
LOC100642836	LOC100642857	LOC100642861	LOC100642885	LOC100642933	LOC100643050
LOC100643059	LOC100643102	LOC100643112	LOC100643114	LOC100643155	LOC100643165
LOC100643170	LOC100643173	LOC100643205	LOC100643215	LOC100643223	LOC100643281
LOC100643314	LOC100643329	LOC100643358	LOC100643366	LOC100643437	LOC100643452
LOC100643479	LOC100643550	LOC100643557	LOC100643568	LOC100643599	LOC100643679
LOC100643681	LOC100643695	LOC100643697	LOC100643711	LOC100643719	LOC100643771
LOC100643795	LOC100643809	LOC100643838	LOC100643927	LOC100643938	LOC100644029
LOC100644065	LOC100644136	LOC100644206	LOC100644218	LOC100644323	LOC100644325
LOC100644350	LOC100644354	LOC100644372	LOC100644435	LOC100644438	LOC100644440
LOC100644466	LOC100644492	LOC100644515	LOC100644530	LOC100644552	LOC100644556
LOC100644628	LOC100644677	LOC100644685	LOC100644688	LOC100644690	LOC100644711
LOC100644721	LOC100644732	LOC100644739	LOC100644741	LOC100644746	LOC100644758
LOC100644765	LOC100644799	LOC100644803	LOC100644878	LOC100644996	LOC100644998
LOC100645044	LOC100645121	LOC100645122	LOC100645124	LOC100645130	LOC100645183
LOC100645187	LOC100645209	LOC100645254	LOC100645261	LOC100645301	LOC100645372
LOC100645484	LOC100645543	LOC100645552	LOC100645563	LOC100645675	LOC100645740
LOC100645746	LOC100645880	LOC100645908	LOC100645921	LOC100645977	LOC100645978
LOC100645981	LOC100645995	LOC100646035	LOC100646037	LOC100646066	LOC100646100
LOC100646136	LOC100646187	LOC100646267	LOC100646303	LOC100646318	LOC100646409
LOC100646550	LOC100646561	LOC100646633	LOC100646661	LOC100646678	LOC100646700
LOC100646744	LOC100646749	LOC100646757	LOC100646801	LOC100646802	LOC100646836
LOC100646853	LOC100646883	LOC100646986	LOC100647000	LOC100647030	LOC100647042
LOC100647074	LOC100647120	LOC100647134	LOC100647222	LOC100647239	LOC100647291
LOC100647308	LOC100647335	LOC100647396	LOC100647494	LOC100647517	LOC100647546
LOC100647555	LOC100647664	LOC100647674	LOC100647693	LOC100647777	LOC100647808
LOC100647822	LOC100647824	LOC100647862	LOC100647876	LOC100647924	LOC100647925
LOC100648035	LOC100648059	LOC100648074	LOC100648090	LOC100648167	LOC100648201
LOC100648205	LOC100648253	LOC100648287	LOC100648300	LOC100648311	LOC100648320
LOC100648429	LOC100648441	LOC100648456	LOC100648462	LOC100648500	LOC100648513
LOC100648522	LOC100648523	LOC100648596	LOC100648643	LOC100648646	LOC100648674
LOC100648687	LOC100648710	LOC100648712	LOC100648746	LOC100648756	LOC100648782
LOC100648826	LOC100648829	LOC100648938	LOC100648974	LOC100648975	LOC100649035
LOC100649067	LOC100649088	LOC100649097	LOC100649108	LOC100649130	LOC100649136
LOC100649198	LOC100649257	LOC100649260	LOC100649277	LOC100649283	LOC100649353

LOC100649365	LOC100649492	LOC100649564	LOC100649565	LOC100649577	LOC100649584
LOC100649698	LOC100649703	LOC100649760	LOC100649811	LOC100649816	LOC100649820
LOC100649871	LOC100649923	LOC100649931	LOC100649935	LOC100649955	LOC100649976
LOC100650041	LOC100650046	LOC100650124	LOC100650141	LOC100650149	LOC100650163
LOC100650244	LOC100650267	LOC100650275	LOC100650290	LOC100650315	LOC100650342
LOC100650395	LOC100650398	LOC100650408	LOC100650411	LOC100650440	LOC100650459
LOC100650470	LOC100650486	LOC100650533	LOC100650589	LOC100650603	LOC100650648
LOC100650651	LOC100650788	LOC100650854	LOC100650857	LOC100650885	LOC100650918
LOC100650962	LOC100651002	LOC100651010	LOC100651015	LOC100651083	LOC100651125
LOC100651127	LOC100651131	LOC100651136	LOC100651199	LOC100651246	LOC100651251
LOC100651336	LOC100651340	LOC100651366	LOC100651375	LOC100651441	LOC100651446
LOC100651451	LOC100651474	LOC100651534	LOC100651570	LOC100651572	LOC100651577
LOC100651591	LOC100651603	LOC100651610	LOC100651623	LOC100651694	LOC100651758
LOC100651821	LOC100651827	LOC100651838	LOC100651843	LOC100651866	LOC100651876
LOC100651887	LOC100651909	LOC100651950	LOC100651986	LOC100651992	LOC100652007
LOC100652196	LOC100652210	LOC100652227	LOC105665781	LOC105665882	LOC105665997
LOC105666169	LOC105666180	LOC105666541	LOC105666639	LOC105666640	LOC105666711
LOC110119154	LOC110119185	LOC110119695	LOC110119803	LOC110119837	LOC110120039
LOC110120321					